Journal of Inorganic and Organometallic Polymers and Materials
https://doi.org/10.1007/s10904-020-01611-9

TOPICAL REVIEWS

A Comprehensive Study on Methods and Materials for Photocatalytic Water Splitting and Hydrogen Production as a Renewable Energy Resource

Muhammad Rafique[1] · Rikza Mubashar[2] · Muneeb Irshad[3] · S. S. A. Gillani[4] · M. Bilal Tahir[2] · N. R. Khalid[2] · Aqsa Yasmin[5] · M. Aamir Shehzad[6]

Received: 24 March 2020 / Accepted: 21 May 2020

Abstract
High energy consumption, rapid increase in its demand and depletion of energy resources in the world are compelling the researchers for exploration of renewable energy resources in order to attain sustain development of nations. Many existing resources are being used to fulfil the current requirements. But these existing resources are also causing serious environmental pollution which is a very serious concern of the current era. Therefore, there is an immense need to think and produce environment friendly and sustainable renewable energy resources. Water, being abundant on Earth, is one of the most suitable sources of hydrogen energy. In this work the splitting of water and hydrogen production by different techniques, specially the promising photocatalysis technique, are discussed in detail. The water splitting and hydrogen production depend upon the properties of photocatalysts which rose from the nature, composition and other factors of photocatalysts. Therefore, this study discussed different materials like metal oxides, metal sulphides, nanocomposites, etc. which are used for photocatalytic hydrogen production. In addition, the pros and cons of the utilized materials are discussed to select the best class of materials for hydrogen production from water splitting. This review will help the beginners of this field to understand the basic mechanisms of different hydrogen production techniques along with their advantages and disadvantages. However, it will also help the field experts and industrialists to select the best class of materials for hydrogen evolution from water splitting.

Keywords Photocatalysis · Water splitting · Hydrogen production · Co-catalyst · Nanocomposites · 2D materials

1 Introduction and Renewable Energy Resources

High energy consumption due to enormous increase in the world population and modern lifestyle are considered as the major reasons of energy crisis [1, 2]. Currently, fossil fuels are playing an important role to fulfill our daily energy consumption needs. About 90% of global energy i.e. industrial energy and transportation energy are derived from fossil fuels [3]. Fossil fuels have gained a lot of interest because of their economic affordability and availability. But, on the other hand, due to their use from hundreds of years they will be depleted in near future [4]. Moreover, burning of fossil fuels lead to emission of greenhouse gases which are polluting our environment and as a result the ozone layer is being severely damaging [5, 6]. Therefore, there is an urgent need for development of renewable, clean and environment friendly energy resource which would help to overcome present global energy issues.

✉ Muhammad Rafique
mrafique.uet@gmail.com; mrafique@uosahiwal.edu.pk; muhammad.rafique@uog.edu.pk

[1] Department of Physics, University of Sahiwal, Sahiwal 57000, Pakistan

[2] Department of Physics, Faculty of Science, University of Gujrat, Gujrat 50700, Pakistan

[3] Department of Physics, University of Engineering and Technology, Lahore, Pakistan

[4] Department of Physics, Government College University, Lahore, Pakistan

[5] Department of Materials and Membrane Technology Center, Punjab Industrial Estate, Kasur, Pakistan

[6] Department of Polymer and Process Engineering, University of Engineering and Technology, Lahore, Pakistan

Published online: 09 June 2020

Researchers have designed many alternate methods for energy production such as hydropower, wind power, geothermal, etc. But these alternative methods have many practical limitations which reduced their efficiency and applicability. Energy produced by wind power is very unreliable which leads the difficulty to manage power systems [7, 8]. Hydropower is also an advanced energy source with practical experience of over 100 years, but, this method has also practical limitations regarding high cost of dams construction [9]. This method has space for more improvement by decreasing surrounding effects, refining operation, and designing more efficient and low cost technological solutions [10, 11]. Geothermal energy is a continuous renewable energy source which uses heat energy of earth interior and hitched due to high cost of development and maintenance. It has negative environmental influence such as polluted air emission, polluting airways and subsidence [11–13]. Another renewable energy resource is the solar energy which is considered as most promising candidate to replace the fossil fuels. Solar energy also leads us to attain clean, sustainable and environment friendly fuel and it is estimated that only 0.01% solar energy conversion can be sufficient to overcome the whole world's energy crisis. The solar cells can be a good source for solar energy conversion, but, lesser energy storage capacity and low efficiency limited their use [14, 15]. Due to practical difficulties of all renewable energy sources, water splitting for hydrogen production has been recognized as a most suitable renewable energy resource.

2 Water Splitting and Hydrogen Production

Hydrogen is considered to be storable and clean energy source for the future [16–18]. The main advantages of using hydrogen as a fuel includes no reliance on fossil fuels, location independence, less area requirement, harmless products, safe, economical, clean and environment friendly fuel [19, 20]. Therefore, recently, a great attention is paid on the finding of different methods for hydrogen production which is being considered most suitable renewable energy resource [21]. Among all hydrogen production methods, the water splitting is gaining immense consideration from the researchers as the most promising method of hydrogen production. Water splitting and different methods of water splitting are explained in the preceding sections along with their pros and cons. Furthermore, the mechanism of water splitting, suitable materials for improving efficiency of water splitting and hence hydrogen production is also discussed.

3 Water Splitting

Water is one of the most plentiful, cheap and unlimited material on the Earth which can act as clean and environment friendly source. Therefore, water splitting is one of the most favorable source for hydrogen production and a renewable energy resource [22–24].

3.1 Thermochemical Water Splitting

Thermochemical water splitting is a method in which water is allowed to heat at a high temperature and resulting in hydrogen and oxygen after the decomposition of water. The high temperature up to 2500 °C is required to turns Gibbs function at zero and hydrogen gets separated from the mixture. This is called single stage water decomposition and is explained in Eq. 1 [24].

$$2H_2O \rightarrow 2H_2 + O_2\,(T > 2500^{\circ}C) \tag{1}$$

High energy is required for this process which cannot be obtained by using conventional and sustainable energy sources. Therefore, a different mechanism was developed to reduce the decomposition temperature of water. The mechanism involves multiple stages, each stage requires lesser temperature and hence overall temperature is decreased, however, efficiency is increased. For example, the decomposition of water by tin oxide is represented by Eqs. 2–3 [24].

$$SnO_2(s) \rightarrow SnO(g) + 0.5O_2\,(T = 1600^{\circ}C) \tag{2}$$

$$SnO(s) + H_2O(g) \rightarrow SnO_2(s) + H_2(g)\,(T = 550^{\circ}C) \tag{3}$$

After passing through different cycles, the temperature is decreased but still high temperature is required for the multi-stage process which is obtained from solar or nuclear energy. Figure 1 illustrates the thermochemical water splitting based on solar light. The main advantage of using this method is that there is no release of greenhouse gases, but, toxicity of elements being used and high cost requirements are the drawbacks of this method [25].

3.2 Photo-Biological Water Splitting

Photo-biological water splitting can be categorized into two major groups, organic photolysis and water photolysis, on the basis of reaction mechanism, resulting products and reactant organisms. Organic photolysis is capable of degrading organic waste-materials and production of high yield hydrogen, but, hazardous byproducts such as CO_2 (environment pollutant) limited this method. Water photolysis is considered as clean and environment friendly reaction as compared to organic photolysis. This method is further categorized in two approaches: direct and indirect water splitting. In direct approach, water is splitted into hydrogen and oxygen through photosynthesis as shown in Fig. 2. The obtained hydrogen ions are then converted into gaseous form by using hydrogenase enzymes. The enzymes are sensitive to oxygen; therefore, low content of oxygen should be maintained. The

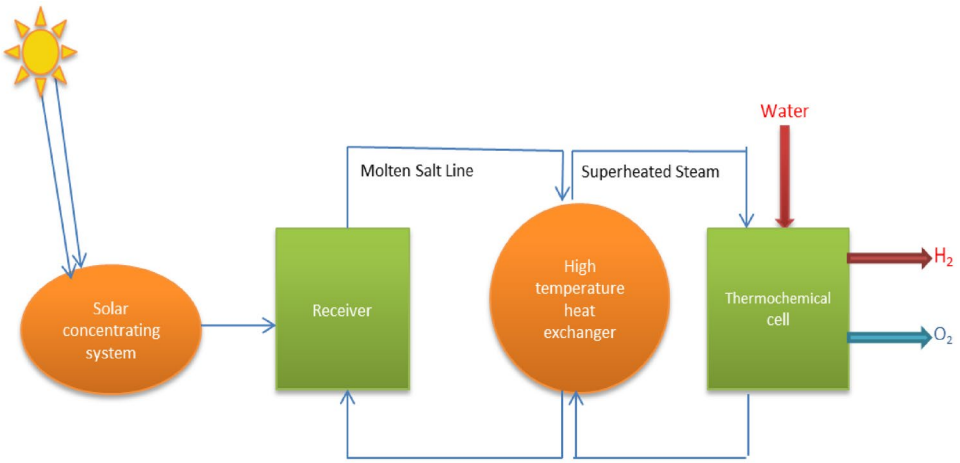

Fig. 1 Schematic diagram of thermochemical process

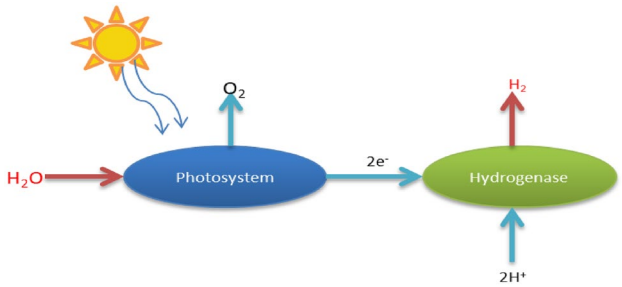

Fig. 2 Schematic diagram of direct photolysis

direct water photolysis using green algae is represented in Eq. 4 [24]. The cost of direct photolysis is too high which is the downside of this approach [24, 26, 27].

$$2H_2O + \text{light energy} \rightarrow 2H_2 + O_2 \quad (4)$$

In indirect photolysis, cyanobacteria or blue-green algae is used for hydrogen production from water which is explained in Eqs. 5 and 6. The schematic representation of indirect bio-photolysis is shown in Fig. 3 [28]. In this approach, hydrogen is produced through hydrogenase and nitrogenase enzymes [29]. The efficiency of both indirect and direct photolysis is comparable but the cost of indirect approach is quite less than direct approach [24].

$$12H_2O + 6CO_2 \rightarrow C_6H_{12}O_6 + 6O_2 \quad (5)$$

$$C_6H_{12}O_6 + 12H_2O \rightarrow 12H_2 + 6CO_2 \quad (6)$$

The shortcomings of using photo-biological water splitting are (i) need of large reactor volume (ii) high cost of raw materials (iii) low hydrogen rates and production and (iv) no waste utilization [30].

3.3 High Temperature Electrolysis Water Splitting

In high temperature electrolysis, water (in the form of steam) is disassociated into hydrogen and oxygen at a high temperature

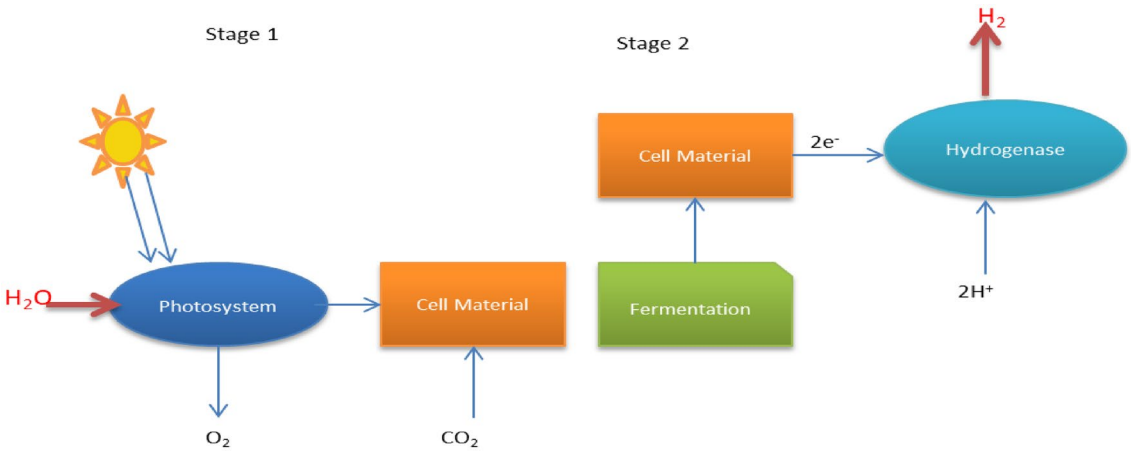

Fig. 3 Schematic diagram of indirect photolysis

of 700–1000 °C. The process is completed in an electrochemical cell consisting of cathode, anode and electrolyte. After dissociation, the hydrogen and oxygen are obtained at negative and positive electrodes, respectively. The chemical reactions that occur on cathode and anode are described in Eqs. 7 and 8 [31–33].

$$\text{At cathode}: \quad H_2O + 2e^- \rightarrow H_2 + O^{2-} \tag{7}$$

$$\text{At anode}: \quad O^{2-} \rightarrow \frac{1}{2}O_2 + 2e^- \tag{8}$$

As the temperature is increased, the efficiency of the method also increases as compare to electrolysis at room temperature. Heat is transferred to the system either by using steam or ultimately using thermal energy which reduces the need of electrical energy. Another benefit of this method is the probability of meeting the zero greenhouse gas emission rates which is the clean source for heating the objects externally. But the major drawback of high temperature electrolysis is the requirement of high temperature. This requirement restricts the components to fulfill specific needs. Other challenges which have to be met to increase the efficiency of hydrogen production using this method include (i) developing an electrolyte with high chemical stability which can have low electrical and high ionic conductivity, (ii) designing the materials which can be chemically stable to the extent to bear the high temperatures and (iii) high porosity of the material [34, 35].

3.4 Photo Electrolysis Water Splitting

Photo electrolysis is a process in which electrodes are exposed to external radiations in compliment with heterogeneous photocatalyst on each or either of the two electrodes. Therefore, chemical energy is produced from these electrical and photonic energies. The hydrogen production from this method can be summarized as (i) a photon having enough energy is allowed to produce electron hole pair, (ii) electrical current is produced (by the movement of electron form anode to cathode), (iii) water is splitted into H^+ and O^-, (iv) gaseous hydrogen is formed at cathode by reduction of proton and (v) resulting gases are separated, processed and stored. The schematic diagram of complete process is represented in Fig. 4. The whole reaction in photo electrolysis is summarized in Eqs. 9–11 [24].

$$\text{Anode}: \quad 2p^+ + H_2O \rightarrow 0.5O_2 + 2H^+ \tag{9}$$

$$\text{Cathode}: \quad 2e^- + 2H^+ \rightarrow H_2 \tag{10}$$

$$\text{Overall}: \quad H_2O \rightarrow H_2 + 0.5O_2 \tag{11}$$

The efficiency of this process depends upon the crystallinity of electrode, corrosion resistance, reactivity and

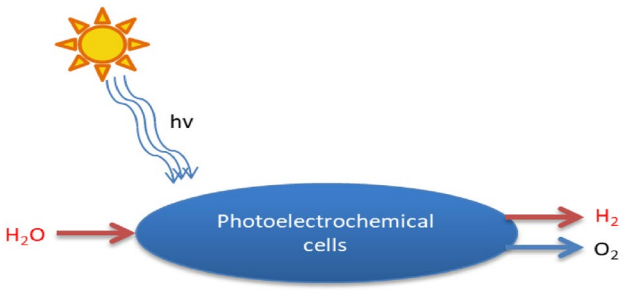

Fig. 4 Schematic diagram of photo electrolysis water splitting

adsorbent material. The disadvantages of using photo electrolysis process are stability of photo electrode and low efficiency of hydrogen production. Moreover, if the efficiency is increased, stability will be compromised and vice versa [34, 36].

3.5 Photocatalytic Water Splitting

Solar energy is freely and endlessly available clean source of energy which can assist to meet present and future energy needs. Thus, the key point here is to harness energy into usable energy. One of the best way to store this energy is photocatalysis which stores energy in the form of chemical fuel [37]. Hence, photocatalysis is defined as a process in which photo catalyst responses to visible light illumination and is vastly used for water splitting and hence hydrogen production. [38]. In addition, this method is also a source for oxygen, CO_2 and CH_4, which are also the fuels for other energy production methods. There are two schemes for the photocatalytic water splitting known as one-step excitation mechanism and the two-step excitation mechanism [39].

In one-step photo-excitation mechanism, photo catalyst is activated under visible light which has appropriate potential to decompose water into O_2 and H_2 as represented in Fig. 5. The photocatalyst should own the properties such as smaller band gap to produce visible photons, stability and thermodynamic potential for water splitting.

It is much hard to fulfill all the necessities in a material which halt the utility of this mechanism [40, 41]. Therefore, the requirements can be met by another approach i.e. two steps photo-excitation system. This method has resemblance with the "natural photosynthesis process" and is known as Z-scheme, as shown in Fig. 6. A wide-ranging availability of visible light and possibility of split-up of evolved the hydrogen and oxygen leads this scheme to be applicable and more successful than one step photo-excitation [42, 43]. When the light of energy equals or more than the band gap energy of photocatalyst is allowed to fall, electron excitation occurs from valance band (VB) to the conduction band (CB), leaving holes in VB. The

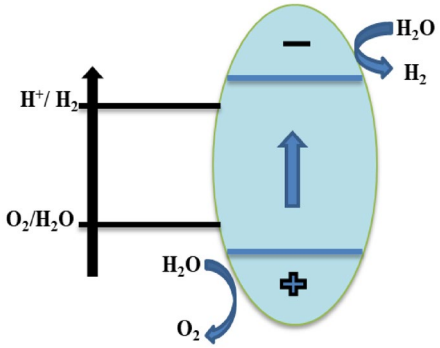

Fig. 5 Illustration of one-step photo-excitation system

process results in reduction and oxidation and is illustrated in Eqs. 12 and 13 [44]. For water splitting, the top of the VB must be more positive than the oxidation potential required for reduction from H_2O to O_2 and the bottom of the CB must be more negative than the reduction potential of H^+ to hydrogen molecule, therefore, minimum photon energy required for the overall reaction is 1.23 eV. But, for the transfer of electron between the molecules of photocatalysts and water, there exist an activation barrier, which needs energy greater than the band gap energy in order to perform photocatalytic water splitting [44, 45].

At PS 1 (Photosystem):

$$H_2O + 2H^+ + \text{reduction} \rightarrow 2H_2 + \text{oxidation} \tag{12}$$

At PS 2 (Photosystem):

$$H_2O + \text{oxidation} \rightarrow O_2 + 2H^+ + \text{reduction} \tag{13}$$

The absence of fossil fuels and no production of carbon dioxide or any other kind of by products are the comprehensions of using photocatalytic water splitting for hydrogen production [46, 47].

The comparison for all the available methods for water splitting refers that each process has its pros and cons. The barrier in the progress of high temperature electrolysis is the stability of catalysts at high temperature. The electrolysis has high probability of side reactions rather than the generation of original product. Thermochemical process enriches toxic effects and high cost. Biological water splitting has disadvantage of large amount of waste products whose reusability is also an issue. In photocatalytic water splitting the efficiency is not high. But the study of literature reveals that this problem can be overcome by fabricating suitable photocatalysts [48]. But, the major advantage of his process is absence of any kind of by product. Additionally, photocatalytic water splitting, being low cost and clean source of water splitting, represents a more attractive process for water splitting [15].

The semiconductor materials are the promising materials with required band gap, therefore, are widely used as photocatalysts [49]. In semiconductor photocatalysis, electronic structure of photocatalyst has crucial importance, consists of lower energy band known as VB and higher energy band known as CB. The gap between CB and VB is called energy band gap, usually under normal condition, electrons reside in VB. When electron gains energy by external source (applying potential across semiconductor or provide thermal energy) it jumps from VB to the CB. In case of semiconductor photocatalyst, external energy is provided by means of visible light illumination. When electron jumps from valance to conduction band, leaves a hole behind and both act like the charge carriers. These electron–hole pair takes part in oxidation and reduction reactions. The complete mechanism for TiO_2 is expressed in Eq. 14 [50].

$$TiO_2 \longrightarrow h\nu e^-_{TiO_2} + h^+_{TiO_2} \tag{14}$$

The photo-generated charge carriers (i.e. electrons and holes) take part in oxidation and reduction reaction which has important role in whole photocatalytic process for

Fig. 6 Illustration of two-step photo excitation system

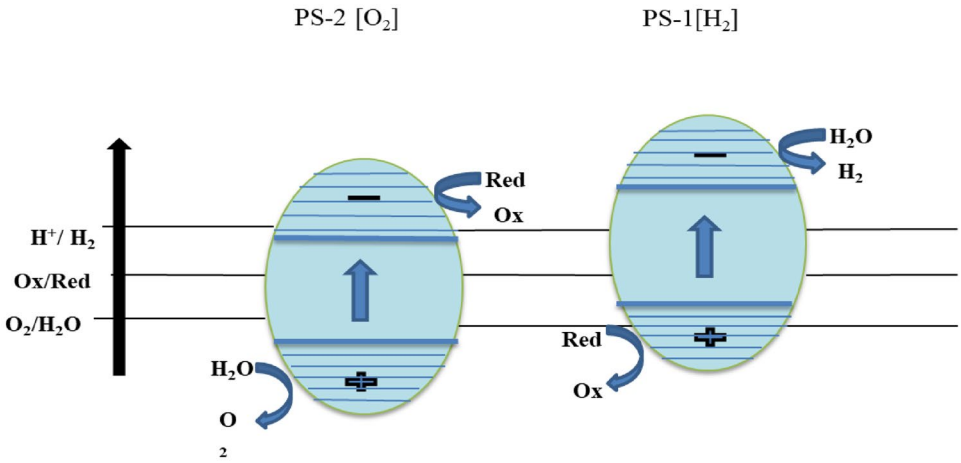

hydrogen production or other beneficial applications. For hydrogen production, CB should be at much negative potential ($\frac{E_{H_2}}{H_2O}$) and VB should be more positive ($\frac{E_{O_2}}{H_2O}$) for proficient O_2 evolution as shown in Fig. 7 below.

4 Hydrogen Production from Photocatalytic Water Splitting

Hydrogen produced from the photocatalytic water splitting plays an important role for the most sustainable renewable energy source [51, 52] because it can be stored, transported easily and converted in electrical energy efficiently. The efficiency of the process can be enhanced by tuning the properties of photocatalysts. The step of excitation and adsorption depends upon the electrical and structural properties of material, the defects and the co-catalysts. The defect in the structure act as recombination centers which decreases the crystallinity and hence reduces the efficiency. The activity of photocatalysts can be intensified by introducing solid co-catalyst. The co-catalysts are deposited on the surface of photocatalyst having size less than 50 nm and are responsible for production of active sites and initiate the hydrogen evolution because most of the photocatalysts don't have ability to activate hydrogen on the surface. Hence, designing the surface as well as bulk properties are necessary for the efficient performance of photocatalysts. The other properties [53] which influence the efficiency of the process are shown in Fig. 8. Therefore, detailed mechanism of photocatalytic water splitting and performance of different materials including semiconductors, nanocomposites, nano-catalysts and 2D materials is explained in the preceding section.

4.1 Mechanism of Photocatalytic Water Splitting

Photocatalysis is a chemical process in which light is allowed to fall on the surface of photocatalyst which results in the production of hydrogen from water (Fig. 9a) [55, 56], conversion of solar light into electrical energy (Fig. 9b) [57, 58], degradation of organic pollutants (Fig. 9c) [59, 60] and reduction of carbon dioxide in organic fuels (Fig. 9d) [61–63]. In photocatalytic water splitting, redox reactions (i.e. oxidation and reduction process to form hydrogen and oxygen) occur on the surface of photocatalyst. This process begins when light is irradiated on the photon absorber (photocatalyst) which results in the creation of an exciton. This results in the separation of electron hole pair which get diffused on the interface. This leads to the transfer of electrons and hole into the reduction and oxidation reaction sites and finally the oxygen and hydrogen is evolved there [64–66]. This process is considered the most sustainable and potential method for meeting the energy needs/crisis [67]. But, in practical implementation, there are two constraints in applying this process. Firstly, photon energy (hυ) should be higher than the band gap energy of catalyst; secondly, reactants should have redox potential between bottom of the conduction (BCB) and top of the valance band (TVB) of photocatalyst. First limitation suggests that the band gap

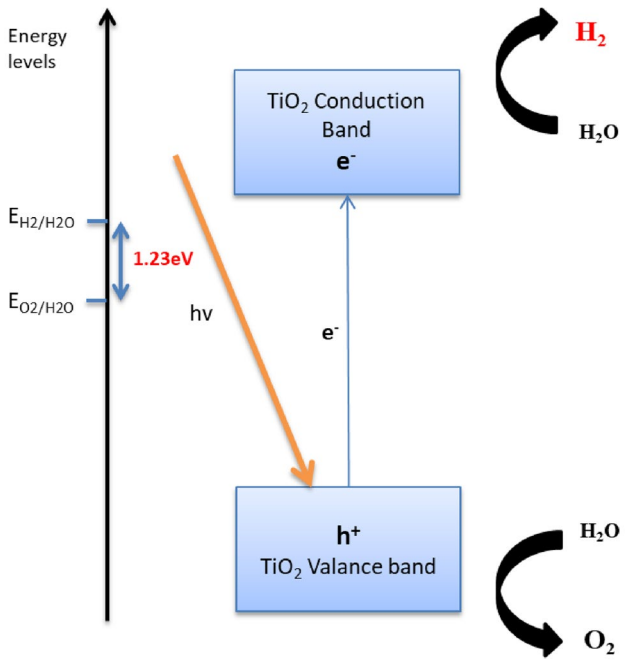

Fig. 7 Photocatalytic water splitting for hydrogen and oxygen evolution by TiO_2

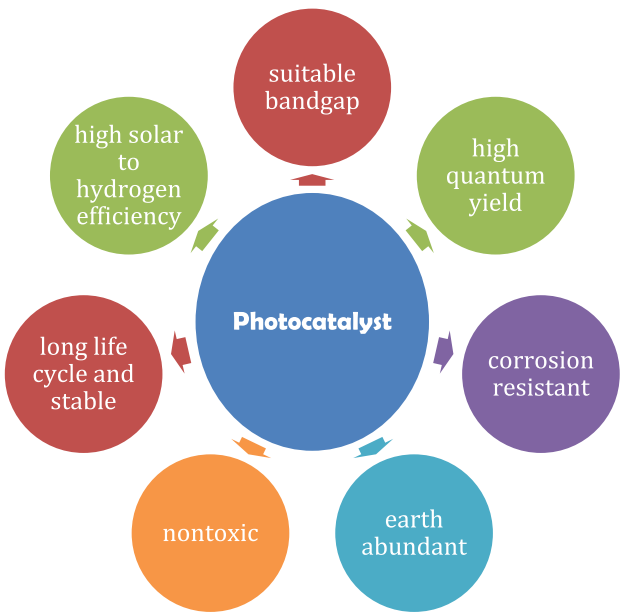

Fig. 8 Parameters influencing the photocatalysts [54]

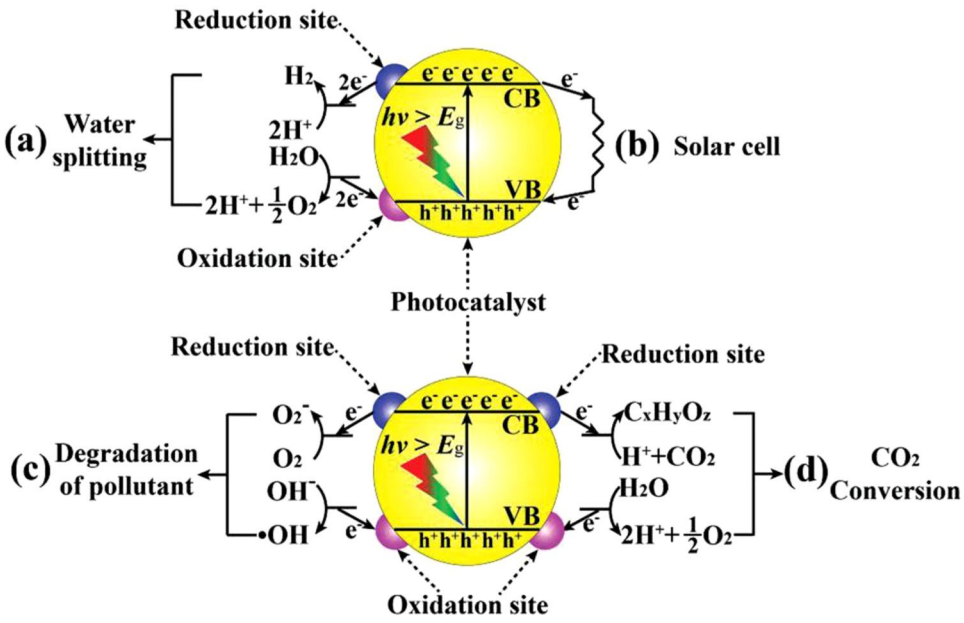

Fig. 9 Photocatalytic water splitting **a** for hydrogen production, **b** conversion of solar light into electrical energy, **c** degradation of pollutants, **d** reduction of carbon dioxide [68]

should be small enough to enhance utilization of solar light (but many photocatalysts have band gap in ultraviolet (UV) region which means that band gap is large). The second constraint is opposite to first which implies that BCB band must be more negative and TVB must be more positive for the efficient oxidation and reduction process. This implies that band gap should be larger, and this will lead to deficient in light absorption. Hence, this process is not suitable for efficient water splitting.

Therefore, another method known as Z-scheme which is based on the natural phenomena of photosynthesis is used for photocatalytic water splitting [69]. The schematic diagram of Z scheme in the form of natural photosynthesis is shown in Fig. 10. The light is allowed to fall on the photocatalyst which excites the electron from highest occupied molecular orbital (HOMO) (photosystem II) to lowest unoccupied molecular orbital (LUMO). The electron moves towards photosystem I (PS I) using electron mediator. These electrons in PS I get excited from HOMO to LUMO and reduces carbon dioxide. The holes present in HOMO photosystem II (PS II) oxidize the water and show high rate oxidation and reduction in PS II and PS I, respectively, and hence richer redox reactions ability. Resultantly, it can be concluded that Z-scheme results in the enhancement of light absorption by combining two band gaps of smaller widths.

In artificial Z scheme, the electron mediator is in the form of paired acceptor/donor (A/D). Figure 11 illustrates the Z-Scheme photocatalytic process in the form of acceptor and donor. There is no physical connection between both photosystems (PS I and PS II). The redox reaction

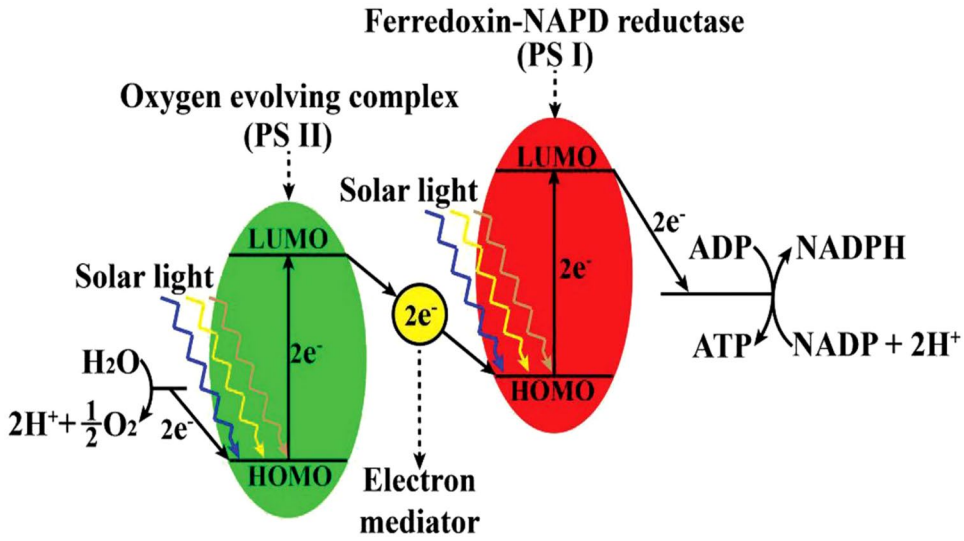

Fig. 10 Z-Scheme photocatalytic process in natural photosynthesis [68]

of paired A/D occurs in the form of electron transfer from the CB of PS II to the VB of PS I. The complete reaction is given in Eqs. 15 and 16 [68].

$$A + e^- \rightarrow D\,(\text{CB of PS II}) \tag{15}$$

$$D + h^+ \rightarrow A\,(\text{VB of PS I}) \tag{16}$$

In first step, the absorption of photogenerated electron from the conduction band of PS II results in the reduction of accepted electron into the donor electron. In second step, the oxidization of resulted donor electron converts into the electron acceptor by photogenerated hole from valance band of PS I. Finally, the holes generated in valance band of PS II and electron generated in conduction band of PS I performs the process of oxidation and reduction respectively [42, 44]. Moreover, the acceptor and donor electrons can also combine with the electrons generated in the CB of PS I and generated holes in the valance band of PS II and are expressed in Eqs. 17 and 18 [68].

$$A + e^- \rightarrow D\,(\text{CB of PS I}) \tag{17}$$

$$D + h^+ \rightarrow A\,(\text{VB of PS II}) \tag{18}$$

The efficiency of photocatalytic water splitting can be enhanced by tuning the properties of photocatalysts. The properties which influence the efficiency of photocatalytic activity are shown in Fig. 8 and are summarized as; Firstly, bandgap of photocatalyst should be comparable with incident light. Secondly, it should be wide enough to avoid recombination rate which limits our application. Thirdly, photo catalyst or hybrid junction photocatalyst should be synthesized in such a way that bandgap should be narrow enough to respond under larger wavelengths of solar light spectrum [70, 71].

4.2 Hydrogen Production Using Semiconducting Materials/Photocatalytic Water Splitting Using Semiconducting Materials

Now a days, hydrogen production using the semiconductor materials is considered to be the most emerging [72] and ideal process for direct solar energy conversion. In hydrogen production, different semiconductor materials are used as photocatalyst which differ from each other in their energy bandgap. The process depends upon the excitation of the electrons and hence bandgap of the catalyst. The bandgap of a photocatalyst is the difference between the highest occupied band VB and lowest CB for the electrons. When suitable light is incident on the photocatalyst, electrons are excited, the excited electrons are combined with bulk or surface causing the energy loss in the form of heat, there is redox reaction of water due to the electrons and holes produced from light, and as a result hydrogen and oxygen is produced [73]. The whole process is illustrated in Fig. 12 below.

There are enormous semiconductors including metal oxides and sulphides, which have been used for the purpose of hydrogen production. Some of the metal oxides and sulphides with their efficiency and other important factors are explained below.

4.2.1 Metal Oxide Photocatalysts

Metal oxides are one of the suitable classes of materials which can be used as a photocatalysts because of their possessions like morphology, high surface area, morphology, band gap etc. [74, 75]. Therefore, many metal oxides are being used as photocatalyst for hydrogen production. Among metal oxides, TiO_2 is widely used photocatalyst for water splitting and hence hydrogen production [48]. In photocatalytic process, TiO_2 is allowed to excite by shining it with light. The energy of light photons should be equal or more than materials bandgap energy. The incident light excites the electron from VB to CB and leaves a hole behind resulting

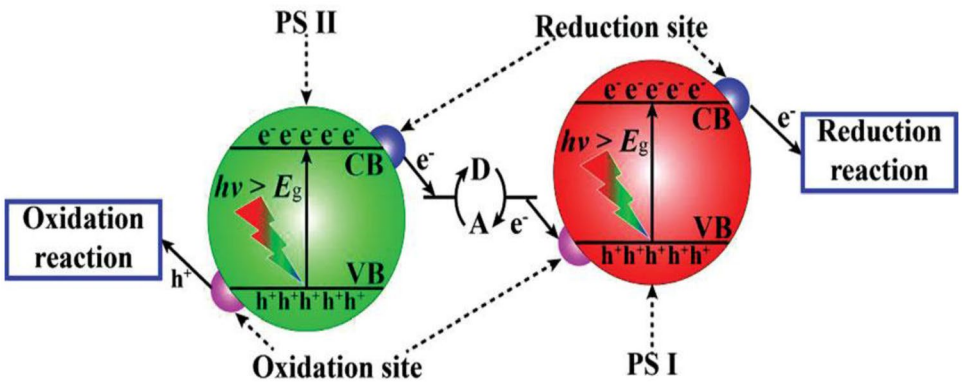

Fig. 11 Illustration of z-scheme photocatalysis for artificial photosynthesis [68]

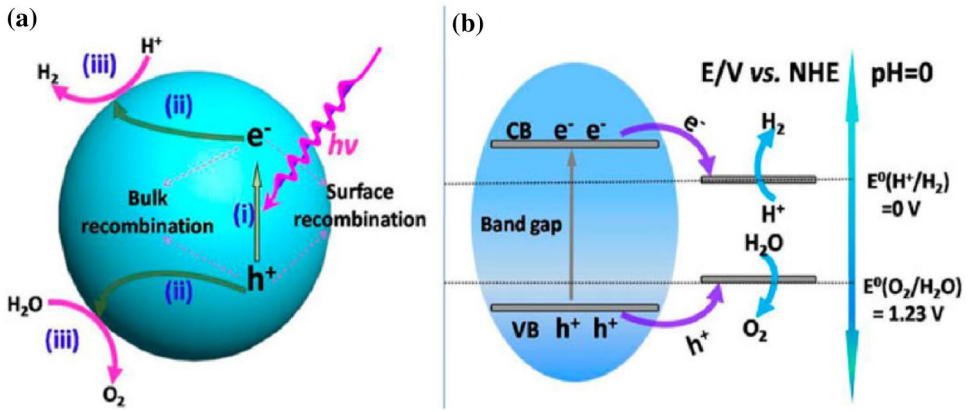

Fig. 12 Hydrogen production using semiconductor materials [73]

in generation of electron–hole pair and the electron–hole pairs may recombine. The efficient photocatalyst utilizes these holes and electrons in reaction rather than recombination. The process become more effective when a metal is introduced which traps the excited electron from the CB and transfer them to the hydrogen ions [76].

Although TiO_2 fulfills many of the good photocatalyst conditions, but still has the drawbacks to become a universal photocatalyst. Firstly, the recombination of electrons in CB occurs with holes in VB and energy is utilized in the form of unwanted heat. Secondly, there is a greater probability of reverse reaction due to decomposition of hydrogen and oxygen. Thirdly, the bandgap of titanium dioxide is 3.2 eV due to which it can only response to the UV-light which is only 4% of the spectrum, whereas the visible light contains 50% of spectrum. Therefore, due to these reasons, the efficiency of TiO_2 is not much high and is still limited for the solar light. There are enormous metal oxides which were reported as a photocatalysts for hydrogen production and some of these are enlisted in Table 1 with their quantum efficiency and other important factors.

Hence, there are large numbers of metal oxides which have been synthesized with different methods, sizes and morphologies [109, 110]. It is concluded that the properties of metal oxides materials can be tuned by changing these properties but still there is a need of investigating other types of materials which can provide oxidation of organic substrates under visible light [111] to increase the quantum efficiency of photocatalysts.

4.2.2 Metal Sulphides Photocatalysts

In past few decades, there are many reports on sulphides based metal catalysts with different sacrificial reagents. From all, some of the metal sulphides catalysts are enlisted in Table 2. According to Zhang and Guo, the metal sulphides are the most suitable photocatalysts for hydrogen production because of their high conduction band position and potential comparable to water potential for hydrogen production. In addition, the metal sulphides have better response under sunlight as compared to the oxides. It is reported that there are more than thirty sulphides materials that can be used as catalysts for hydrogen production. The overview confirmed that all these sulphides photocatalysts comprise of metal cations having d^{10} configuration and are shown in Fig. 13.

It is notable that the conduction band of these materials is made up of d and sp orbitals and the valence bands relate to the 3p orbitals. The difference between both bands is O 2p orbitals. The configuration shows that CB has enough negative potential to reduce water into hydrogen and narrower the bandgap to visible solar spectrum.

According to the genealogy in Fig. 14, sulphides catalysts are grouped according to the composition and formulation of material like IIB-VIA, IIB-IIIA, IA-IIIA and IB-IIB-IVA-VIA sulphides photocatalysts. All these photocatalyst are considered as the different types of zinc blend structure by substituting the IIB atoms with other metals. However, due to the substitution of different metallic elements, the symmetry of the resulting crystal structure is reduced. This is the reason that tetragonal crystal systems are represented in sulphides such as chalcopyrite structure and stannite structures and its symmetry is visibly lower than the cubic systems [73, 112].

Metal sulphides can be the promising photocatalysts but photo-corrosion is the key issue on the way to their high performance [113]. Therefore, sacrificial reagents are required that can provide photogenerated electrons to consume photogenerated holes to avoid anodic photocorrosion. But this cannot be the eventual solution for the stability of metal sulphides photocatalysts [112]. This problem requires the designing of appropriate z-scheme heterojunction so that photo corrosion can be prevented. Moreover the charge transfer route and photocatalytic mechanism of these materials is not well explained [114].

Table 1 Metal oxides for photocatalytic water-splitting for hydrogen production

Photocatalyst	Synthesis method	Mass (g)	Incident light	Efficiency/quantum yield	Hydrogen production $\mu molh^{-1}\ g^{-1}$	References
TiO_2:Ga	Solvothermal method	1.5	Pyrex filter		20.86	[77]
TiO_2:Ni	Hydrothermal method	0.3	Pyrex filter		566.7	[78]
TiO_2:Sc	Hydrolysis, calcination	0.1	Pyrex filter		7500	[79]
TiO_2:Pr	Hydrolysis, calcination	0.1	Pyrex filter		6600	[79]
TiO_2:Sn/Eu	Polyol method	0.2	Quartz filter	40.4	92	[80]
TiO_2/CuO	Impregnation method	1	Quartz filter		18,500	[81–83]
$SrTiO_3/TiO_2$	Solid state reaction	0.1			560	[84]
B/Ti oxide	Sol–gel method	0.3	Quartz filter		73	[85, 86]
$Sr_3Ti_2O_7$	Polymerized complex method	1	Quartz filter		144	[87]
$Sr_4Ti_3O_{10}$	Polymerized complex method	1	Quartz filter	4.5 at 360 nm	170	[88]
$Rb_{1.5}La_2Ti_{2.5}Nb_{0.5}O_{10}$	Solid state reaction	1	Quartz filter		725	[89]
$Rb_2La_2Ti_3O_{10}$	Solid state reaction	1	Quartz filter	5 at 330 nm	869	[89]
$KaLaZr_{0.3}Ti_{0.7}O_4$	Two step on exchange reaction	0.3	Quartz filter	12.5	766.7	[90]
$La_4CaTi_5O_{17}$	Solid state reaction	1	Quartz filter	20 at less than 320 nm	499	[91]
$BaLa_4Ti_4O_{15}$	Polymerized complex method	0.5	Quartz filter	15 at 270 nm	4600	[92]
$Y_2Ti_2O_7$	Polymerized complex method	0.5	Quartz filter	6 at 313 nm	2000	[93–95]
$Cs_2Ti_2O_5$	Solid state reaction	1	Quartz filter		500	[96]
$Zr_2(PO_4)PVX_3$	Hydrothermal method	0.025	< 320 nm	4 at less than 320 nm	267.8	[97]
$Ba_5Nb_4O_{15}$	Polymerized complex method	0.5	Quartz filter	17 at 270 nm	8042	[92, 98]
$H_2LaNb_2O_7$:In	Solid-state reaction	1	>290 nm	1.54 at less than 290 nm	5268	[99]
$NaTaO_3$	Solid state reaction	1	Quartz filter	56 at 270 nm	19,800	[100, 101]
$SrTa_2O_6$	Solid state reaction	1	Quartz filter	7 at 270 nm	960	[102, 103]
$Sr_2Ta_2O_7$	Polymerized complex method	0.7	Quartz filter	24 at 270 nm	5024	[104–107]
$K_2Sr_{1.5}Ta_3O_{10}$	Solid state reaction	0.5	Pyrex filter	2 at 252.5 nm	200	[108]

4.2.3 Co-catalyst

The enhancement of photocatalytic water splitting can be done in different ways. Among all, one method is the surface modification by loading metals or metal oxides nanoparticles [115]. These loaded metals or metal oxide nanoparticles are known as co-catalysts [116]. The effect of different noble metal co-catalysts on photocatalytic activities of CdS powders have been examined [117]. It was reported that Pt and Rh^- doped cadmium sulphides showed much better activities. The reber and his co-workers testified a chain of notable hydrogen production efficiencies which are about 34%, 25% and 16% in $S^{2-}/H_2PO_2^-$, S^{2-}/SO_3^{2-} and Na_2S aqueous solutions, respectively, at temperature of 60 °C. Borgarello and his co-workers [76] placed small amounts of ruthenium dioxide (RuO_2) on CdS to result a high quantum yield of H_2 (i.e. 35%) due to hole transfer from VB of CdS to sulphides solution. Tungsten carbide as co-catalyst (platinum like material) was also described to entertain as an outstanding co-catalyst for photocatalytic H_2 production for CdS under visible light [112].

Recently, different compounds of transition metals, generally metal sulphides, are proven to be outstanding co-catalysts for photocatalytic hydrogen evolution particularly CdS. Zong et al. studied the significance CdS loaded by the MoS_2 on photocatalytic activity. The activity of MoS_2/CdS was more than those of CdS when loaded with different noble metals due to the activation energy of hydrogen of MoS_2. Zhang and his co-workers prepared active NiS/CdS photocatalyst as an innovative catalyst using hydrothermal method and reported 51.3% high quantum efficiency in lactic acid-sacrificial solution under 420 nm light irradiation. Additionally, the most promising accomplishment was completed by H. J. Yan and C. Li to describe the about the natural photosynthesis with 93% quantum efficiency under 420 nm light irradiation. Further, CdS particles were decorated with PdS and Pt to act as oxidation and reduction co-catalysts, respectively, as shown in Fig. 15. Other various co-catalysts used for hydrogen production are enlisted in Table 2 along with their quantum efficiency, hydrogen production and other parameters.

4.3 Hydrogen Production Using Nano-catalyst Materials

Hydrogen production from water splitting is a technique which utilizes energy of wind, oceans, sun or waves

Table 2 Various metal sulphides and co-catalysts for photocatalytic water splitting/hydrogen production

Photocatalyst	Mass (g)	Incident light (nm)	Co-catalyst	Quantum yield (%)	Morphology	Synthesis method	Activity ($\mu molg^{-1} h^{-1}$)	References
CdS	0.1	UV	Pt		Particles	Precipitation method	6000	[119]
CdS	0.1	> 420	WC		Particles	Hydrothermal	1350	[120]
CdS	0.5	> 420	Pt	19.7	Particles	Poly inorganic solid-state reaction method	7856	[121]
CdS	0.05	> 420	Pt	13.9	Nanorods	Solvothermal method	4603.2	[122]
CdS/Alumina	2	Complete spectrum				Impregnation method	180.8	[123]
CdS/Alumina	2	Complete spectrum				Impregnation method	41.3	[124]
CdS/Ag_2S	0.1	Complete spectrum	Pt		Nanosheets + Nanorods	Two-step precipitation method	874	[125]
CdS/MgO	0.5	Complete spectrum	Pt		Particles	Etching method	290	[126]
$CdS/LaMnO_3$	0.1	>420			Particles	Reverse Micelle method	595	[127]
CdS/MoO_3		> 400		28.82 at 420 nm	Core (MoO_3), Shell (CdS)	Sonochemistry	5250	[128]
CdS/TiO_2	0.1	> 450	Pt	13.4 at > 450 nm		Sol–Gel method	8.4	[129]
CdS/TiO_2	0.1	> 420	Pt		Particles (TiO_2 nano + CdS bulk)	Two step method	4224	[130]
CdS/TiO_2	0.1	420	Pt		Particles	Precipitation/sol–gel method	6400	[131]
CdS/TiO_2 NTs	0.15	> 420	Pt	43.3 at 420 nm	Nanoparticles and Nanotubes	Ultrasonic stirring method	2680	[132]
CdS/ZnO	0.2		RuO_2		Coreshell nanorods	A teo step method	6200	[133]
CdZnS	0.1	< 400		2.17 at UV	Particles	Co-precipitation method	16,320	[134]
CdS/Zeolite		> 330	ZnS			Ion Exchange and sulfidation	2455	[135]
CdS–ZnO–CdO	0.2	Visible light	Ru		Coreshell nanorods	Sequential precipitation method	75	[133]
$Cd_{0.5}Zn_{0.5}S$	0.1	> 420	Pt			Hydrothermal method	350	[136]
$Cd0_{0.1}Zn_{0.5}S$-CNT	0.05	> 420		7.9 at 40 nm	Particles	Hydrothermal method	1563.2	[137]
CdS.ZnS		> 400		1.86 at 404 nm	ZnS coated CdS	ZnS precipitated on CdS		[138]
CdS.ZnS	0.0413	Sunlight				Coprecipitation method	2283.9	[139]
CdS/ZnS/n–Si	0.1					Coprecipitation method	1584.8	[140]

Table 2 (continued)

Photocatalyst	Mass (g)	Incident light (nm)	Co-catalyst	Quantum yield (%)	Morphology	Synthesis method	Activity ($\mu molg^{-1} h^{-1}$)	References
$ZnIn_2S_4$	0.1	Visible light			Nanosheets made up of flowerlike microspheres	CPBr assisted hydrothermal method	766.8	[141]
$ZnIn_2S_4$	0.2	> 430	Pt	18.4 at 420 nm	Microspheres with some petals	Hydrothermal method	562.25	[142]
$ZnIn_2S_4$/MWCNTs	0.1	> 420		23.3 at 420 nm	Flower like microspheres made up of many interleaving flakes	Facile hydrothermal method	6840	[143]
Ba doped CdZnS	0.2	> 430		17.4 at 425 nm	Nanoparticles	Thermal sulfurication method	700	[144]
$CdIn_2S_4$	0.5	> 420			Microspheres made up of nanopetals	Surfactant assisted hydrothermal method	6476	[145]
$CdIn_2S_4$	0.5	> 420		17.1 at 500 nm	Microspheres made up of nanopetals and nanotubes		6960	[146]
$AgGaS_2$	0.1	> 420	Pt		Particles	Coprecipitation and annealing method	3000	[147]
$AgIn_5S_8$	0.3	> 420	Pt	5.3 at 411.2 nm		Coprecipitation and heat treatment	133.3	[148]
Copper doped ZnS	0.2	Overall spectrum			Shell structure particles	Sulfidation and ion exchange	210	[149]
$CuGa_3S_5$	0.05	> 420	Rh NiS Pt	1.3 at 420–520 nm	Particles	Coprecipitation and heat treated method	800 1000 3000	[150]

[151–154]. The hydrogen production from water splitting in a sustainable way requires an artificial photosynthetic system and cheap, stable, environment friendly and efficient catalyst in order to oxidize water [155–158]. In nature, the only system available for catalyzing water oxidation is water oxidizing complex (WOC) of PSII in which WOC consists of Mn_4O_5Ca cluster and PSII having a protein environment which manage the movement of protons, access water and reaction coordinates.

The structure of manganese-calcium cluster at atomic resolution was reported by Shen et al. which is presented in Fig. 16. The structure contains one calcium and four manganese clusters linked with five oxygen atoms. It is also clear that the structure has four water-molecules among which two molecules support the water oxidation [159–161]. Furthermore, manganese complexes are used as catalysts for oxygen evolution. In 1987, Kaneko et al. described the adsorption of di-nuclear complex on kaolin clay surface as catalyst for water oxidation. In solution the Manganese Schiff base complex used as biomimetic catalyst for oxygen producing complex. Gobi et al. described the oxidation of water by manganese schiff base complexes in the presence of cerium. They also reported on the ligand (NO_2, Br) electron withdrawing substituent boosted the reactivity of the complexes towards oxygen production [162].

Mn_4O_5Ca cluster has a dimension approximately equal to 0.5 nm exhibited good structural and functional properties and is used in PS-II model. Moreover, as to be nano catalyst showed high surface area and hence high active sites on the surface and acts as water oxidizing catalyst. Dehydrogenation for the production of ultra-pure H_2 with some contamination is produced in fuel cell by Pt as catalyst. The reaction mechanism is shown in Eqs. 19–20 [162].

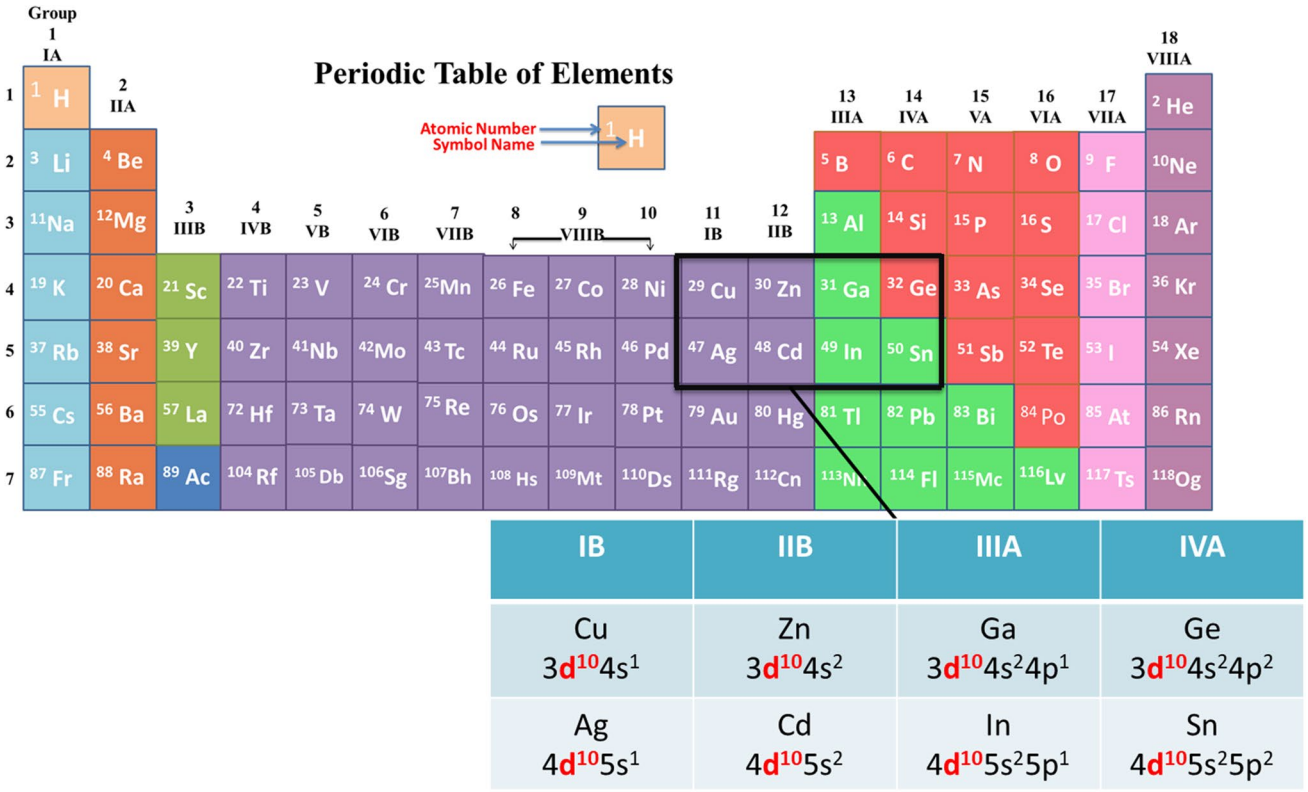

Fig. 13 Commonly used elements in sulphides photocatalysts for hydrogen production

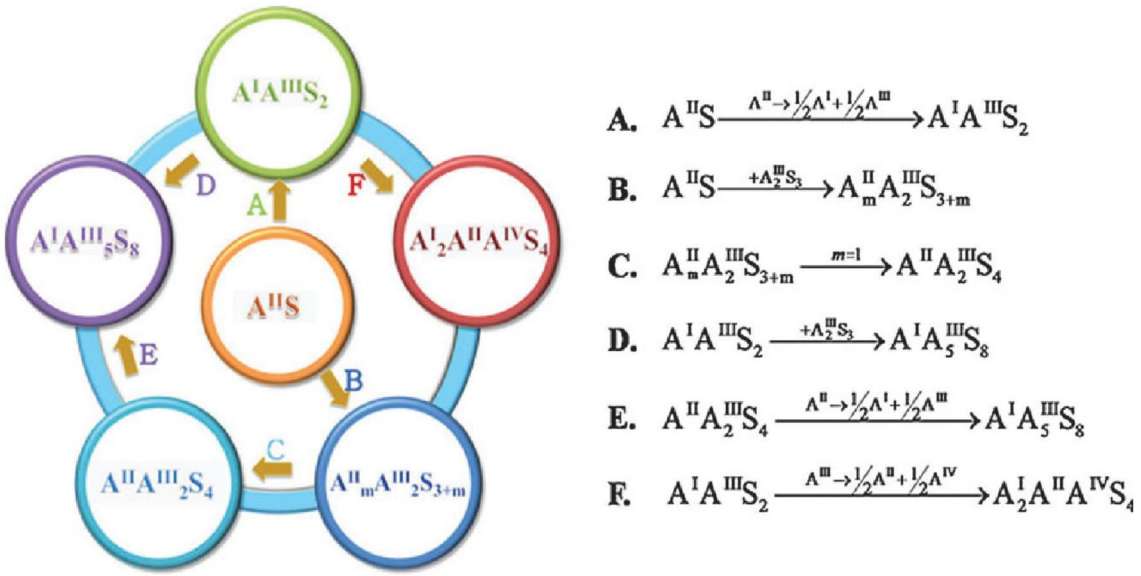

Fig. 14 Genealogy of sulphides photocatalysts [112]

$$HCOOH \rightarrow H_2 + CO_2 \quad \text{where,} \quad \Delta G = -48.4\,\text{kJ/mol} \tag{19}$$

$$HCOOH \rightarrow H_2O + CO \quad \text{where,} \quad \Delta G = -28.5\ \text{kJ/mol} \tag{20}$$

The homogeneous catalysts were used for decomposition of formic acid but are limited in device fabrication. Therefore, attention is paid on the fabrication of practical heterogeneous catalysts that can exhibit enhanced activity under ambient conditions. The performance of these catalysts is

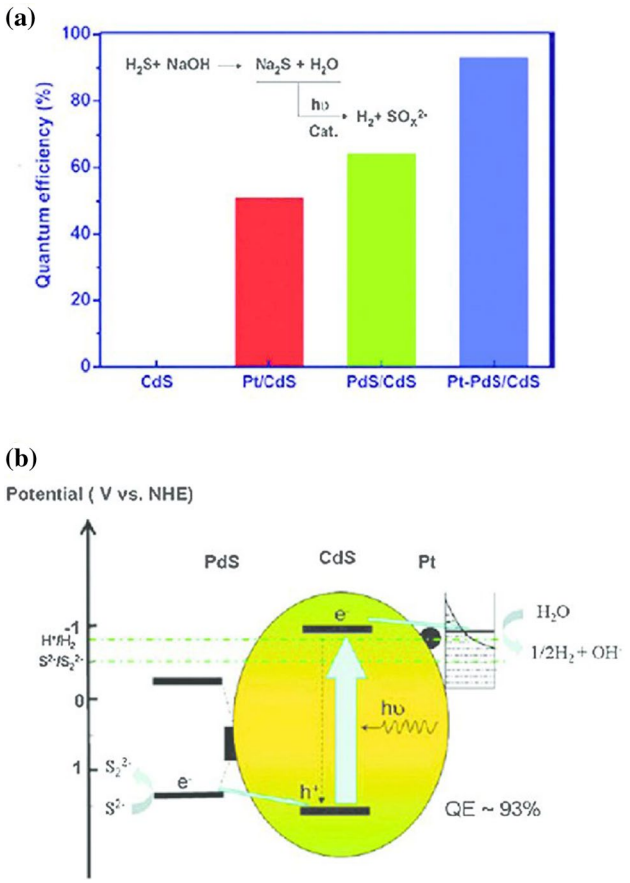

Fig. 15 **a** Apparent quantum yield. **b** Change transmission mechanism during photocatalytic reaction [112, 118]

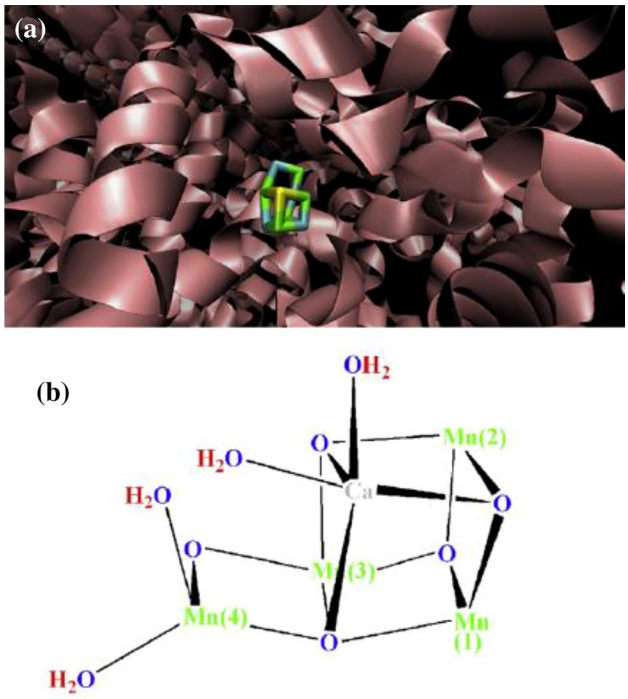

Fig. 16 **a** The Mn_4O_5Ca cluster in Photosystem II, **b** manganese calcium cluster whereas ribbons denotes the surrounding proteins [162]

also limited due to severe reaction conditions. Afterwards, the attention was focused to "Raisins" which have exceptional properties including the hydrophobic or hydrophilic characteristics and can easily introduce range of fundamental groups and their capability to swell in a reaction. For commercial use, the Pd nano-catalysts can be prepared from resins available commercially like Haas, Rohm, Amberlite, etc. [163]. The palladium supported resins were expected to show high activity and are shown in Table 3.

4.4 Hydrogen Production Using Nanocomposite Materials

Metal oxide nanomaterials being highly stable, less toxic and cheap are of great importance [164, 165]. The major utilization of these materials is in photocatalytic process where solar energy is consumed to split the water for Hydrogen energy production. In photocatalytic process, the key factor is the band gap and the mostly metal oxides are only activated under UV light which is a small fraction of the solar spectrum. On the other hand, some other metal oxides have suitable energy bandgap for effective absorption in solar spectrum, but, have smaller diffusion lengths and hence are inefficient for photocatalytic activity. Therefore, there is immense need of the metal oxides which can be efficient under visible light and can also have suitable bandgaps. To fulfill this need, great attention is paid on the fabrication of metal oxide nanocomposites which are expected potential solution, hence, a variety of nanocomposites are being fabricated and are being performing the task [166].

One of the most suitable composite materials is titanium dioxide and carbon nanotubes (TiO_2/CNTs) in which electrons are transferred to CNTs and holes stayed on TiO_2 which avoids and reduces the recombination. This composite also has high surface to volume ratio which increases the adsorption rate and hence can be used as photosensitizers. Additionally, the bonding between titanium, oxygen and carbon also supports the photocatalytic mechanism. Furthermore, carbon nanotubes are found to be effective for controlling the morphology of titanium dioxide nanoparticles.

A 2D carbon nanosheet, named as graphene, possesses unique properties because of its large surface area (practically up to 2600 m^2/g), mobile charge carriers and excellent mechanical strength [167–169]. Kamat et al. [170] studied the photocatalytic activity of graphene and reported that when electrons from TiO_2 are transferred to graphene oxide, convert it into reduced graphene oxide (RGO). Another research group claimed that TiO_2 (P25)–RGO composites are highly efficient for photocatalytic activity and can

Table 3 Textural properties of palladium supported resins [163]

Catalyst	Mixture	Functional group	Exchange capacity (meq/mL)	Property	Water absorption capacity (%)	Average size (mm)	Hydrogen Production µmol
Pd/mixture 1	200CTNa	SO_3H	Greater than 1.8	Highly acidic	46 to 51	5.1	16
Pd/mixture 2	FPC3500	COOH	Greater than 2.0	Weakly acidic	60 to 70	2.1	22
Pd/mixture 3	IRA96SB	NMe_2	Greater than 1.3	Weakly basic	57 to 63	1.7	96
Pd/mixture 4	IRA900JCI	NMe_2Cl	Greater than 1.0	Highly basic	56 to 66	5.8	40

degrade methylene blue efficiently. Cui and his co-workers claimed that if TiO_2 –RGO composite is prepared using sol–gel method in the solution where Na_2S and Na_2SO_3 are surface agents, the hydrogen production occurs and the formation rate is doubled or even more i.e. 8.6 µmolh^{-1} compared to 4.5 µmolh^{-1} with P25. A comparison of P25 and its composite materials in the presence of methanol aqueous solution for the hydrogen evolution process is shown in Fig. 17a. It was also showed that hydrothermal method is the most preferred method whereas the hydrazine is least one as shown in Fig. 17b. Furthermore, it can be concluded that RGO based composite material is more suitable for hydrogen evolution among all these composites.

Another example of composite material used for hydrogen production is CdS–GO. The physical and chemical properties of GO (graphene oxide) make it quite suitable to be coupled with CdS for improved efficiency. The hydrogen evolution occurs because the lowest energy state of GO's conduction band is higher than the energy required for the hydrogen evolution process, but can be further enhanced by using a co-catalyst. Li et al. used CdS cluster decorated with graphene and loaded with 0.5 wt% Pt (co-catalyst) as photocatalyst for hydrogen production. An apparent quantum yield of 22.5% was obtained with visible light of wavelength 420 nm. Different methods were used for preparation of this composite material.

Another study revealed that CdS coupled with different carbonaceous materials not only act as supporting material and electrons acceptor, but, it is also a low cost efficient co-catalyst for hydrogen evolution [172]. The technique used for the preparation of nanocomposite was facile precipitation. Visible light with sacrificial agents Na_2S or Na_2SO_3 were utilized. It was also noticed that there is increase in the photocatalytic activity of CdS–GO as compared to the bared CdS under visible light and the evolution rate was measured to be 314 µmolh^{-1}. Hence, it can is evident that the composite material can be used as a cheap, efficient and abundant photocatalysts for the

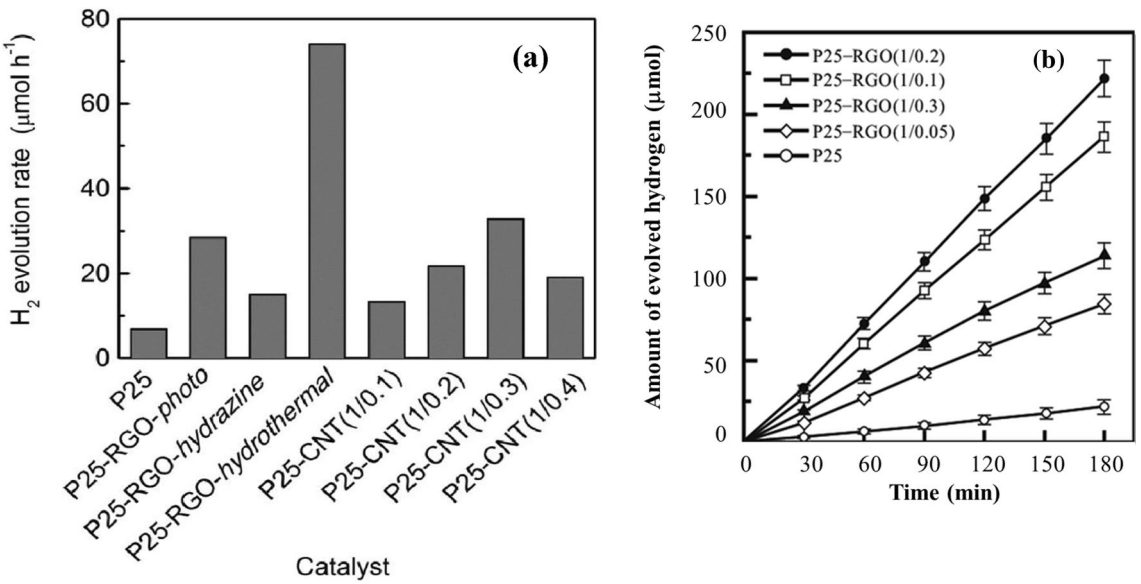

Fig. 17 **a** A comparison between the photocatalytic activity of P25, P25-CNT (with different mass ratios) and P25–RGO (with different mass ratio). **b** Photocatalytic performances of P25–RGO-hydrothermal series for the evolution of H_2 [171]

hydrogen evolution process [172]. Some other examples of nanocomposites used for hydrogen production activity are enlisted in Table 4.

4.5 Hydrogen Production by Using 2D Materials

Recently, Transition Metal Dichalcogenides (TMDs) have gained a lot of attention because of their large surface area, various surface states and tunable electrical properties [185] i.e. two dimensional (2D) thin sheets of the atomic size. The 2D structure of TMDs exhibits the unique physical, chemical and mechanical properties [186] and hence makes them suitable for use in electronics and optoelectronic devices [187, 188]. Many semiconducting materials like MoX_2 or WX_2 (X = Se, S, etc.) have their band gaps near to UV light and can be tuned to visible range on the basis of their atomic layers thickness [189, 190]. As the thickness of molybdenum disulfide's (MoS_2) layer is decreased, there is red or blue shift depending on wavenumber which can be elucidated on the basis of van der Waal interactions among different planes [190]. This leads to the change of indirect band gap of MoS_2 from 1.29 eV to 1.90 eV whereas only 0.1 eV of change in direct band gap occurs. As a consequence of this behavior, the band undergoes a crossover from indirect band gap to direct bandgap [191]. For a material of thickness less than 1 nm, the sunlight spectrum absorption is 10% which is stronger than any commonly used semiconductors [192].

It is reported that MoS_2 is a suitable material as a photocatalyst in Hydro-Desulfurization (HDS) reactions. The results showed that adsorption occur at the edges of TMDs. The photocatalytic activity strongly depends on the adsorption energy (ΔG_{H^*}) which directly affects the reactivity as shown in Fig. 18. A catalytic reaction is efficient when the interaction of catalysts and reactants is neither too strong nor too weak. If ΔG_{H^*} is strong then desorption and conversion will be slow which tends to poison the surface of chemical. On the other hand, if free energy is high then the reaction is rate limited by adsorption of reactant due to inefficient binding. The theoretical calculations performed by Hinnemann and his co-workers revealed that MoS_2 can be a promising catalyst for hydrogen evolution reaction [193]. Similar results were also presented by electrochemical calculations on graphite based MoS_2 particles.

The calculation of free energy of adsorption revealed that best edge configuration of Mo occurred for 50% S (ΔG_{H^*} = 0.06 eV) as compared to 100% S (ΔG_{H^*} = − 0.45 eV) [195]. Furthermore, different experiments also showed that

Table 4 Various nanocomposites for hydrogen production

Photocatalyst	Synthesis method	Morphology	Incident light	Efficiency/ quantum yield	Hydrogen production $\mu molh^{-1} g^{-1}$	References
GO–TiO_2	Two step oxidations	Core–shell structure	UV-irradiation		50 $\mu molh^{-1}$	[173]
ZnS–Graphene oxide	Two-step wet chemistry process	2D sheet and micrometer sized wrinkles	Visible light			[174]
(RGO)–$Zn_{0.8}Cd_{0.2}S$	Co-precipitation-hydrothermal reduction strategy	Nanoparticles	Visible light	23.4	1824	[175]
($Ru/SrTiO_3$:Rh)–(PRGO/$BiVO_4$)	Chemical reduction process		Visible light		4.8 µmol	[176]
CdS–Ag_2S	Microwave assisted solvothermal method and ion exchange strategy	Nanosheets and Nanoparticles	Visible light		375.6	[177]
CuS/TiO_2	Hydrothermal and solution based process	Nanoflakes and Nanospindles	Visible light		1262	[178]
(rGO/$InVO_2$–TiO_2)	Hydrothermal process	Nanoparticles	UV- irradiation		1669 $\mu molh^{-1}$	[179]
Au/TiO_2	One-step process	TiO_2 network with embedded gold nanoparticles	UV			[180]
$ZnIn_2S_4$@NH_2-MIL-125(Ti)	Solvothermal method	Nanosheets	Visible light	4.3	2204.2 µmol g^{-1}	[181]
ZnO/$CoMoO_4$	Refluxing and calcination process	Nano fringes	UV			[182]
(gCN/M/AgW/AgBr)	Co-deposition	Nanosheets and Nanoparticles	Visible light			[183]
CdS/TiO_2	Electrospinning and Photo-deposition	Nanofibers	Visible light			[184]

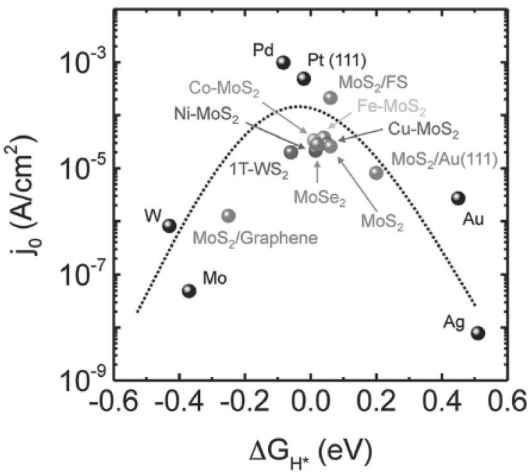

Fig. 18 Hydrogen adsorption on 2D TMDs [194]

MoS_2 as a catalyst can perform the reaction with materials below than noble metals as shown in Fig. 19. Hence, to enhance the catalytic activity of the materials, the conducting edges should be increased. It has also been proved that edge sites perform more fast electrochemical reaction than basal planes [196].

Some other suitable materials for catalytic activities are sulfur and selenium based TMDs where similar behavior, as mention above, is expected for these materials. There are two main factors for electrocatalysis: catalytic activity and stability of active sites. The stability directly depends upon the ΔG_{H-X} of H–X (X = S or Se) as the desorption becomes favorable at $\Delta G_{H-X} > 0$. The relation between energy of hydrogen adsorption and ΔG_{H-X} is inverse and when $\Delta G_{H-X} > 0$ there is a less stable catalyst and strong hydrogen binding occurs ($\Delta G_{H^*} < 0$). Tsai and his co-workers calculated the free energy for both hydrogen adsorption and H–X adsorption to check the stability of edges and basal planes of different 2D TMDs as shown in Fig. 19a. It was observed that the stability of active basal planes of semiconductor material is significantly higher than metallic TMDs. It refers that TMDs having active basal planes ($\Delta G_{H^*} \approx 0$) are also more stable [197]. Hence, it can be concluded that basal planes can be used for controlling the catalytic activity with free energy of hydrogen adsorption as shown in Fig. 19b.

Some other examples of 2D materials for photocatalytic hydrogen production with their hydrogen production efficiency are enlisted in Table 5. Hence, we conclude that for increasing the catalytic activity of TMDs, designing the 2D TMDs structure is quite effective and useful. The promising properties of 2D materials can be used to avoid the recombination of electron–hole pairs, to harvest sunlight efficiently and to drive the electrons to active sites for enhancement in catalytic reaction [194].

5 Challenges and Future Prospect

The hydrogen production efficiency in photocatalytic water splitting majorly depends upon the properties of photocatalyst like low cost, suitable bandgap, stability and high production ability. The metal oxides based photocatalysts are widely used because of their distinctive properties for water catalysis, but, are limited due to their band gap in UV range (small fraction of solar spectrum) and smaller diffusion lengths. The limitations are compromised by doping, nanocomposites, co-catalysts and 2D material fabrication. The nanocomposites are used where band gaps are tuned to

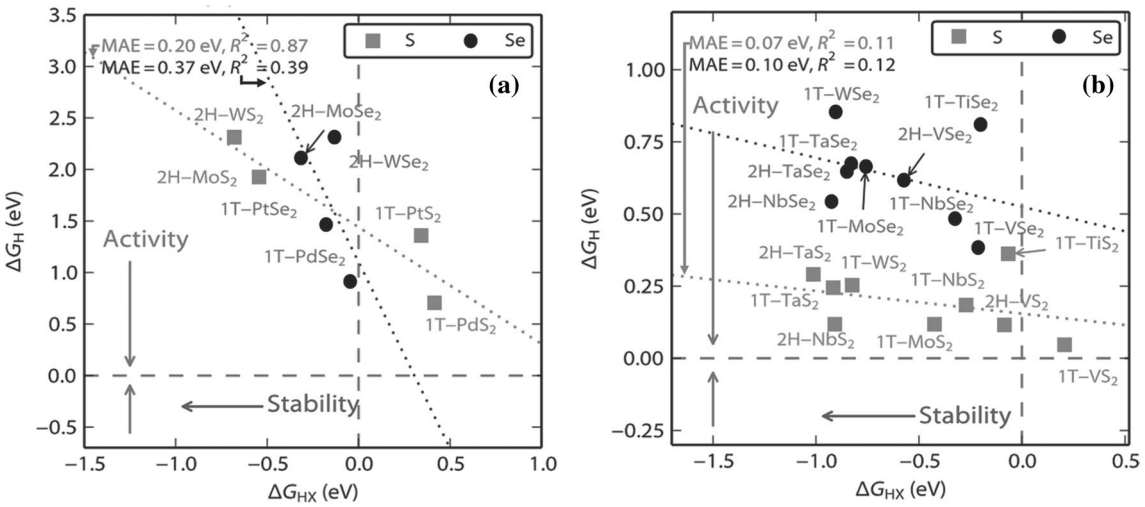

Fig. 19 **a** Hydrogen adsorption for semiconducting TMDs. **b** In general the stronger binding of X, the greater stability of TMDs, the lower the reactivity of TMDs, the weaker the hydrogen binding [194]

Table 5 Some examples of 2D photocatalysts for hydrogen production

Photocatalyst	Synthesis method	Morphology	Incident light	Efficiency/quantum yield	Hydrogen production $\mu molh^{-1} g^{-1}$	References
Ti_2C and g-C_3N_4	Thermal process + selective etching	Coral like structure			47.5 µmol h^{-1}	[198]
CdSe-MoS_2	Two step chemical method	Nano ribbons and nanosheets	Visible light	9.2% at 440 nm	890	[199]
WS_2/CdS	Impregnation and solidification method	Nanoparticles and nanosheets	Visible light	5.0% at 420 nm	4200	[200]
ZnS–WS_2/CdS	Ball milling and calcination method	Particles	Visible light		12,240	[201]
MoS_2–CdS	Hot injection method	Nanohybrid	Visible light		1472	[202]
$Zn_{0.2}Cd_{0.8}S/MoS_2$	Photo assisted deposition method	Nanoparticles and nanosheets	Visible light		420	[203]
$MoS_2/ZnIn_2S_4$	Solvothermal method	Nanosheets	Visible light		ca.1000	[204]
In_2S_3/MoS_2/CdS	Hydrothermal method	Nanorods and nanoparticles	Visible light		1563	[205]
MoS_2/TiO_2	Bal milling	Nanoparticles and Nanosheets	250–380 nm		753.5	[141]
TiO_2/1T-WS_2	Colloidal synthesis method	Nanoparticles and nanosheets	AM 1.5		2570	[206]
TiO_2/MoS_2/G	Hydrothermal method	Nanoparticles and nanosheets		9.7% at 365 nm	2066	[56]
MoS_2/G	Pyrolysis	Nanoparticles and nanosheets	390 nm	1% at 500 nm	ca. 1200	[207]
MoS_2/RGO	Hydrothermal method	Sheets	> 400 nm	24% at 460 nm	4190	[208]
WS_2/mpg-CN	Impregnation and sulfidation	Mesoporous particles	> 420 nm		240	[209]

visible spectrum instead of UV light. Whereas, 2D materials have gained a lot of attention because of their high catalytic activity and low cost. The progress is made in 2D materials where structure and thickness of layer tune the band gap of the catalyst to visible spectra for high hydrogen production rate. But, these materials are limited in practical applications because of aggregation produced during light exposure which reduce the number of active sites. Currently, research is focused on the synthesis and effect of different types of doped, composite and layered materials. However, there are limited investigations on improvement of mechanisms involved in the catalytic activity for hydrogen production. Therefore, the careful investigation on the enhancement in mechanisms and synthesis can lead to a breakthrough in improving the efficiency of the hydrogen production as well as commercialization of the process.

6 Conclusion

Photocatalytic solar light driven water splitting is considered a promising technique for hydrogen production as a renewable energy source which is also a clean, efficient and sustainable renewable energy source. This review presents the comparison of different hydrogen production methods and the most suitable photocatalytic water splitting method. The efficiency is restricted due to limited properties of the photo-catalysts; therefore, researchers have paid attention to design efficient and visible light responsive photocatalysts to enhance solar hydrogen conversion efficiency. The limitations of the widely used metal oxide based photocatalysts are addressed by doping, co-catalysts, nanocomposites and 2D materials. Among all photo-catalysts, 2D materials are the most emerging materials considered in experimental and theoretical approaches. It is expected in near future that 2D materials will pave from laboratory work to industrial scale. The discussion about the methods and materials for water splitting persuades that photocatalytic water splitting with suitable photocatalysts will be the topmost priority to produce the hydrogen as fuel to meet the energy crisis in future.

Compliance with Ethical Standards

Conflict of interest I (we) certify that there is no conflict of interest with any financial organization regarding the material discussed in the manuscript.

References

1. T. Hisatomi, K. Domen, Introductory lecture: sunlight-driven water splitting and carbon dioxide reduction by heterogeneous semiconductor systems as key processes in artificial photosynthesis. Faraday Discuss. **198**, 11–35 (2017)
2. I. Roger, M.A. Shipman, M.D. Symes, Earth-abundant catalysts for electrochemical and photoelectrochemical water splitting. Nat. Rev. Chem. **1**(1), 0003 (2017)
3. A. Ferreira et al., Economic overview of the use and production of photovoltaic solar energy in brazil. Renew. Sustain. Energy Rev. **81**, 181–191 (2018)
4. M.I. Jamesh, Y. Kuang, X. Sun, Constructing earth-abundant 3D nanoarrays for efficient overall water splitting—a review. ChemCatChem **11**(6), 1550–1575 (2019)
5. S.J. Davis, K. Caldeira, Consumption-based accounting of CO_2 emissions. Proc. Natl. Acad. Sci. **107**(12), 5687–5692 (2010)
6. C. Acar, I. Dincer, C. Zamfirescu, A review on selected heterogeneous photocatalysts for hydrogen production. Int. J. Energy Res. **38**(15), 1903–1920 (2014)
7. P.S. Georgilakis, Technical challenges associated with the integration of wind power into power systems. Renew. Sustain. Energy Rev. **12**(3), 852–863 (2008)
8. F. Díaz-González et al., A review of energy storage technologies for wind power applications. Renew. Sustain. Energy Rev. **16**(4), 2154–2171 (2012)
9. A.L. Hamilton, G.W. Characklis, P.M. Reed, Managing financial risk tradeoffs for hydropower generation using snowpack-based index contracts. 2020
10. O. Edenhofer et al., *Renewable energy sources and climate change mitigation: special report of the intergovernmental panel on climate change* (Cambridge University Press, Cambridge, 2011)
11. O. Ellabban, H. Abu-Rub, F. Blaabjerg, Renewable energy resources: current status, future prospects and their enabling technology. Renew. Sustain. Energy Rev. **39**, 748–764 (2014)
12. E. Barbier, Geothermal energy technology and current status: an overview. Renew. Sustain. Energy Rev. **6**(1–2), 3–65 (2002)
13. I.B. Fridleifsson, Geothermal energy for the benefit of the people. Renew. Sustain. Energy Rev. **5**(3), 299–312 (2001)
14. J.A. Turner, Sustainable hydrogen production. Science **305**(5686), 972–974 (2004)
15. I. Dincer, C. Acar, Review and evaluation of hydrogen production methods for better sustainability. Int. J. Hydrog. Energy **40**(34), 11094–11111 (2015)
16. Y. Chen et al., Engineering the atomic interface with single platinum atoms for enhanced photocatalytic hydrogen production. Angew. Chem. Int. Ed. **59**(3), 1295–1301 (2020)
17. R. Chen et al., Integration of lanthanide–transition-metal clusters onto cds surfaces for photocatalytic hydrogen evolution. Angew. Chem. Int. Ed. **57**(51), 16796–16800 (2018)
18. K. Edalati et al., Enhanced photocatalytic hydrogen production on GaN–ZnO oxynitride by introduction of strain-induced nitrogen vacancy complexes. Acta Mater. **185**, 149–156 (2020)
19. C.-H. Liao, C.-W. Huang, J. Wu, Hydrogen production from semiconductor-based photocatalysis via water splitting. Catalysts **2**(4), 490–516 (2012)
20. F. Safari, I. Dincer, A review and comparative evaluation of thermochemical water splitting cycles for hydrogen production. Energy Convers. Manag. **205**, 112182 (2020)
21. J.H. Kim et al., Toward practical solar hydrogen production–an artificial photosynthetic leaf-to-farm challenge. Chem. Soc. Rev. **48**(7), 1908–1971 (2019)
22. Y. Zhang et al., Electrolysis of the Bunsen reaction and properties of the membrane in the sulfur–iodine thermochemical cycle. Ind. Eng. Chem. Res. **53**(35), 13581–13588 (2014)
23. A. Steinfeld, Solar thermochemical production of hydrogen—a review. Sol. Energy **78**(5), 603–615 (2005)
24. P. Nikolaidis, A. Poullikkas, A comparative overview of hydrogen production processes. Renew. Sustain. Energy Rev. **67**, 597–611 (2017)
25. J.E. Funk, Thermochemical hydrogen production: past and present. Int. J. Hydrog. Energy **26**(3), 185–190 (2001)
26. D. Das, N. Khanna, N.T. Veziroğlu, Recent developments in biological hydrogen production processes. Chem. Ind. Chem. Eng. Q. **14**(2), 57–67 (2008)
27. Y. Guan et al., Two-stage photo-biological production of hydrogen by marine green alga *Platymonas subcordiformis*. Biochem. Eng. J. **19**(1), 69–73 (2004)
28. M. Ni et al., An overview of hydrogen production from biomass. Fuel Process. Technol. **87**(5), 461–472 (2006)
29. I.K. Kapdan, F. Kargi, Bio-hydrogen production from waste materials. Enzyme Microb. Technol. **38**(5), 569–582 (2006)
30. J.D. Holladay et al., An overview of hydrogen production technologies. Catal. Today **139**(4), 244–260 (2009)
31. S. Dutta, J. Morehouse, J. Khan, Numerical analysis of laminar flow and heat transfer in a high temperature electrolyzer. Int. J. Hydrog. Energy **22**(9), 883–895 (1997)
32. V. Utgikar, T. Thiesen, Life cycle assessment of high temperature electrolysis for hydrogen production via nuclear energy. Int. J. Hydrog. Energy **31**(7), 939–944 (2006)
33. G. Sandstede, Status of technology and development in water electrolysis. Dechema Monographien **125**, 329–355 (1992)
34. C. Acar, I. Dincer, G.F. Naterer, Review of photocatalytic water-splitting methods for sustainable hydrogen production. Int. J. Energy Res. **40**(11), 1449–1473 (2016)
35. S. Fujiwara et al., Hydrogen production by high temperature electrolysis with nuclear reactor. Prog. Nucl. Energy **50**(2–6), 422–426 (2008)
36. V. Aroutiounian, V. Arakelyan, G. Shahnazaryan, Metal oxide photoelectrodes for hydrogen generation using solar radiation-driven water splitting. Sol. Energy **78**(5), 581–592 (2005)
37. Y. Miseki, K. Sayama, Photocatalytic water splitting for solar hydrogen production using the carbonate effect and the Z-scheme reaction. Adv. Energy Mater. **9**(23), 1801294 (2019)
38. T. Takata, K. Domen, Particulate photocatalysts for water splitting. Recent advances and future prospects. ACS Energy Lett. **4**, 542–549 (2019)
39. A.J. Bard, Photoelectrochemistry and heterogeneous photocatalysis at semiconductors. J. Photochem. **10**(1), 59–75 (1979)
40. K. Maeda et al., GaN: ZnO solid solution as a photocatalyst for visible-light-driven overall water splitting. J. Am. Chem. Soc. **127**(23), 8286–8287 (2005)
41. Y. Lee et al., Zinc germanium oxynitride as a photocatalyst for overall water splitting under visible light. J. Phys. Chem. C **111**(2), 1042–1048 (2007)
42. K. Sayama et al., Stoichiometric water splitting into H_2 and O_2 using a mixture of two different photocatalysts and an IO3−/I− shuttle redox mediator under visible light irradiation. Chem. Commun. **23**, 2416–2417 (2001)
43. H. Kato et al., Construction of Z-scheme type heterogeneous photocatalysis systems for water splitting into H_2 and O_2 under visible light irradiation. Chem. Lett. **33**(10), 1348–1349 (2004)
44. K. Sayama et al., A new photocatalytic water splitting system under visible light irradiation mimicking a Z-scheme mechanism in photosynthesis. J. Photochem. Photobiol. A **148**(1–3), 71–77 (2002)

45. K. Maeda, Photocatalytic water splitting using semiconductor particles: history and recent developments. J. Photochem. Photobiol. C **12**(4), 237–268 (2011)
46. W.J. Youngblood et al., Visible light water splitting using dye-sensitized oxide semiconductors. Acc. Chem. Res. **42**(12), 1966–1973 (2009)
47. A. Kudo, Y. Miseki, Heterogeneous photocatalyst materials for water splitting. Chem. Soc. Rev. **38**(1), 253–278 (2009)
48. Y.-C. Chen et al., Photocatalytic enhancement of hydrogen production in water splitting under simulated solar light by band gap engineering and localized surface plasmon resonance of $Zn_xCd_{1-x}S$ nanowires decorated by Au nanoparticles. Nano Energy **67**, 104225 (2020)
49. N. Khalid et al., Highly visible light responsive metal loaded N/TiO_2 nanoparticles for photocatalytic conversion of CO_2 into methane. Ceram. Int. **43**(9), 6771–6777 (2017)
50. M. Ni et al., A review and recent developments in photocatalytic water-splitting using TiO_2 for hydrogen production. Renew. Sustain. Energy Rev. **11**(3), 401–425 (2007)
51. D. Gao et al., Core-shell Ag@ Ni cocatalyst on the TiO_2 photocatalyst: one-step photoinduced deposition and its improved H2-evolution activity. Appl. Catal. B **260**, 118190 (2020)
52. G. Nabi et al., *Gallium vacancies role in hydrogen storage of single-crystalline GaN hexagonal micro-sheets* (J. Hydrog. Energy, Int, 2020). https://doi.org/10.1016/j.ijhydene.2019.12.042
53. M. Rafique et al., Investigation of photocatalytic and seed germination effects of TiO_2 nanoparticles synthesized by *Melia azedarach* L. leaf extract. J. Inorg. Organomet. Polym. Mater. **29**(6), 2133–2144 (2019)
54. R.D. Tentu, S. Basu, Photocatalytic water splitting for hydrogen production. Curr. Opin. Electrochem. **5**, 56–62 (2017)
55. M.G. Kibria et al., One-step overall water splitting under visible light using multiband InGaN/GaN nanowire heterostructures. ACS Nano **7**(9), 7886–7893 (2013)
56. Q. Xiang, J. Yu, M. Jaroniec, Synergetic effect of MoS_2 and graphene as cocatalysts for enhanced photocatalytic H_2 production activity of TiO_2 nanoparticles. J. Am. Chem. Soc. **134**(15), 6575–6578 (2012)
57. J.A. Christians, R.C. Fung, P.V. Kamat, An inorganic hole conductor for organo-lead halide perovskite solar cells. Improved hole conductivity with copper iodide. J. Am. Chem. Soc. **136**(2), 758–764 (2013)
58. Q. Zhang et al., Nanomaterials for energy conversion and storage. Chem. Soc. Rev. **42**(7), 3127–3171 (2013)
59. J. Yu, X. Yu, Hydrothermal synthesis and photocatalytic activity of zinc oxide hollow spheres. Environ. Sci. Technol. **42**(13), 4902–4907 (2008)
60. Y. Bi et al., Facet effect of single-crystalline Ag_3PO_4 sub-microcrystals on photocatalytic properties. J. Am. Chem. Soc. **133**(17), 6490–6492 (2011)
61. E.V. Kondratenko et al., Status and perspectives of CO_2 conversion into fuels and chemicals by catalytic, photocatalytic and electrocatalytic processes. Energy Environ. Sci. **6**(11), 3112–3135 (2013)
62. S.C. Roy et al., Toward solar fuels: photocatalytic conversion of carbon dioxide to hydrocarbons. ACS Nano **4**(3), 1259–1278 (2010)
63. A. Dhakshinamoorthy et al., Photocatalytic CO_2 reduction by TiO_2 and related titanium containing solids. Energy Environ. Sci. **5**(11), 9217–9233 (2012)
64. T. Shinagawa, K. Takanabe, Towards versatile and sustainable hydrogen production through electrocatalytic water splitting: electrolyte engineering. Chemsuschem **10**(7), 1318–1336 (2017)
65. T. Hisatomi, K. Takanabe, K. Domen, Photocatalytic water-splitting reaction from catalytic and kinetic perspectives. Catal. Lett. **145**(1), 95–108 (2015)
66. K. Takanabe, Solar water splitting using semiconductor photocatalyst powders, in *Solar Energy for Fuels* (Springer, Berlin, 2015), pp. 73–103
67. C. Noda et al., Synthesis of three-component C_3N_4/rGO/C-TiO_2 photocatalyst with enhanced visible-light responsive photocatalytic deNOx activity. Chem. Eng. J. (2020). https://doi.org/10.1016/j.cej.2020.124616
68. P. Zhou, J. Yu, M. Jaroniec, All-solid-state Z-scheme photocatalytic systems. Adv. Mater. **26**(29), 4920–4935 (2014)
69. S. Chen et al., Metal selenide photocatalysts for visible-light-driven Z-scheme pure water splitting. J. Mater. Chem. A **7**, 7415–7422 (2019)
70. S. Shen et al., Visible-light-driven photocatalytic water splitting on nanostructured semiconducting materials. Int. J. Nanotechnol. **8**(6–7), 523–591 (2011)
71. M.R. Gholipour et al., Nanocomposite heterojunctions as sunlight-driven photocatalysts for hydrogen production from water splitting. Nanoscale **7**(18), 8187–8208 (2015)
72. S. Sampath, K. Sellappa, Visible-light-driven photocatalysts for hydrogen production by water splitting. Energy Sources Part A: Recovery Util. Environ. Effects **42**(6), 719–729 (2020)
73. L. Yuan et al., Photocatalytic water splitting for solar hydrogen generation: fundamentals and recent advancements. Int. Rev. Phys. Chem. **35**(1), 1–36 (2016)
74. E. Pelizzetti, C. Minero, Metal oxides as photocatalysts for environmental detoxification. Comments Inorg. Chem. **15**(5–6), 297–337 (1994)
75. T. Hisatomi, J. Kubota, K. Domen, Recent advances in semiconductors for photocatalytic and photoelectrochemical water splitting. Chem. Soc. Rev. **43**(22), 7520–7535 (2014)
76. E. Borgarello et al., Visible light induced generation of hydrogen from H_2S in CdS-dispersions, hole transfer catalysis by RuO_2. Helv. Chim. Acta **65**(1), 243–248 (1982)
77. J. Chae et al., Hydrogen production from photo splitting of water using the Ga-incorporated TiO_2s prepared by a solvothermal method and their characteristics. Bull. Korean Chem. Soc. **30**(2), 302–308 (2009)
78. D. Jing, Y. Zhang, L. Guo, Study on the synthesis of Ni doped mesoporous TiO_2 and its photocatalytic activity for hydrogen evolution in aqueous methanol solution. Chem. Phys. Lett. **415**(1–3), 74–78 (2005)
79. M. Zalas, M. Laniecki, Photocatalytic hydrogen generation over lanthanides-doped titania. Sol. Energy Mater. Sol. Cells **89**(2–3), 287–296 (2005)
80. R. Sasikala et al., Enhanced photocatalytic hydrogen evolution over nanometer sized Sn and Eu doped titanium oxide. Int. J. Hydrog. Energy **33**(19), 4966–4973 (2008)
81. S. Xu, D.D. Sun, Significant improvement of photocatalytic hydrogen generation rate over TiO_2 with deposited CuO. Int. J. Hydrog. Energy **34**(15), 6096–6104 (2009)
82. S. Xu et al., Fabrication and comparison of highly efficient Cu incorporated TiO_2 photocatalyst for hydrogen generation from water. Int. J. Hydrog. Energy **35**(11), 5254–5261 (2010)
83. H.-J. Choi, M. Kang, Hydrogen production from methanol/water decomposition in a liquid photosystem using the anatase structure of Cu loaded TiO_2. Int. J. Hydrog. Energy **32**(16), 3841–3848 (2007)
84. B. Zieliñska, E. Borowiak-Palen, R.J. Kalenczuk, Photocatalytic hydrogen generation over alkaline-earth titanates in the presence of electron donors. Int. J. Hydrog. Energy **33**(7), 1797–1802 (2008)

85. S.-C. Moon et al., Stoichiometric decomposition of pure water over Pt-loaded Ti/B binary oxide under UV-irradiation. Chem. Lett. **27**(2), 117–118 (1998)
86. S.-C. Moon et al., Photocatalytic production of hydrogen from water using TiO_2 and B/TiO_2. Catal. Today **58**(2–3), 125–132 (2000)
87. H. Jeong et al., Hydrogen production by the photocatalytic overall water splitting on $NiO/Sr_3Ti_2O_7$: effect of preparation method. Int. J. Hydrog. Energy **31**(9), 1142–1146 (2006)
88. Y.-G. Ko, W.Y. Lee, Effects of nickel-loading method on the water-splitting activity of a layered $NiO_x/Sr_4Ti_3O_{10}$ photocatalyst. Catal. Lett. **83**(3–4), 157–160 (2002)
89. T. Takata et al., Photocatalytic decomposition of water on spontaneously hydrated layered perovskites. Chem. Mater. **9**(5), 1063–1064 (1997)
90. V.R. Reddy, D.W. Hwang, J.S. Lee, Effect of Zr substitution for Ti in $KLaTiO_4$ for photocatalytic water splitting. Catal. Lett. **90**(1–2), 39–43 (2003)
91. H.G. Kim et al., Highly donor-doped (110) layered perovskite materials as novel photocatalysts for overall water splitting. Chem. Commun. **12**, 1077–1078 (1999)
92. Y. Miseki, H. Kato, A. Kudo, Water splitting into H_2 and O_2 over niobate and titanate photocatalysts with (111) plane-type layered perovskite structure. Energy Environ. Sci. **2**(3), 306–314 (2009)
93. R. Abe et al., Photocatalytic water splitting into H_2 and O_2 over R2Ti2O7 (R = Y, rare earth) with pyrochlore structure. Chem. Lett. **33**(8), 954–955 (2004)
94. M. Higashi et al., Improvement of photocatalytic activity of titanate pyrochlore $Y_2Ti_2O_7$ by addition of excess Y. Chem. Lett. **34**(8), 1122–1123 (2005)
95. R. Abe et al., Photocatalytic activity of R_3MO_7 and $R_2Ti_2O_7$ (R = Y, Gd, La; M = Nb, Ta) for water splitting into H_2 and O_2. J. Phys. Chem. B **110**(5), 2219–2226 (2006)
96. A. Kudo, T. Kondo, Photoluminescent and photocatalytic properties of layered caesiumtitanates, Cs_2TinO_{2n+1} (n = 2, 5, 6). J. Mater. Chem. **7**(5), 777–780 (1997)
97. H. Byrd et al., Crystal structure of a porous zirconium phosphate/phosphonate compound and photocatalytic hydrogen production from related materials. Chem. Mater. **8**(9), 2239–2246 (1996)
98. Y. Miseki, H. Kato, A. Kudo, Water splitting into H_2 and O_2 over $Ba_5Nb_4O_{15}$ photocatalysts with layered perovskite structure prepared by polymerizable complex method. Chem. Lett. **35**(9), 1052–1053 (2006)
99. Y. Wei et al., Photocatalytic water splitting with In-doped $H_2LaNb_2O_7$ composite oxide semiconductors. Sol. Energy Mater. Sol. Cells **93**(8), 1176–1181 (2009)
100. H. Kato, K. Asakura, A. Kudo, Highly efficient water splitting into H_2 and O_2 over lanthanum-doped $NaTaO_3$ photocatalysts with high crystallinity and surface nanostructure. J. Am. Chem. Soc. **125**(10), 3082–3089 (2003)
101. A. Kudo, H. Kato, Effect of lanthanide-doping into $NaTaO_3$ photocatalysts for efficient water splitting. Chem. Phys. Lett. **331**(5–6), 373–377 (2000)
102. H. Kato, A. Kudo, Photocatalytic water splitting into H_2 and O_2 over various tantalate photocatalysts. Catal. Today **78**(1–4), 561–569 (2003)
103. H. Kato, A. Kudo, Photocatalytic decomposition of pure water into H_2 and O_2 over $SrTa_2O_6$ prepared by a flux method. Chem. Lett. **28**(11), 1207–1208 (1999)
104. K. Yoshioka et al., The relationship between photocatalytic activity and crystal structure in strontium tantalates. J. Catal. **232**(1), 102–107 (2005)
105. M. Yoshino et al., Polymerizable complex synthesis of pure $Sr_2Nb_xTa_{2-x}O_7$ solid solutions with high photocatalytic activities for water decomposition into H_2 and O_2. Chem. Mater. **14**(8), 3369–3376 (2002)
106. H. Kato, A. Kudo, Energy structure and photocatalytic activity for water splitting of Sr_2 $(Ta_{1-X}Nb_X)$ $2O_7$ solid solution. J. Photochem. Photobiol. A **145**(1–2), 129–133 (2001)
107. A. Kudo, H. Kato, S. Nakagawa, Water splitting into H_2 and O_2 on new $Sr_2M_2O_7$ (M = Nb and Ta) photocatalysts with layered perovskite structures: factors affecting the photocatalytic activity. J. Phys. Chem. B **104**(3), 571–575 (2000)
108. K. Kalyanasundaram et al., Cleavage of water by visible-light irradiation of colloidal CdS solutions; inhibition of photocorrosion by RuO_2. Angew. Chem. Int. Ed. Engl. **20**(11), 987–988 (1981)
109. H. Wang, A.L. Rogach, Hierarchical SnO_2 nanostructures: recent advances in design, synthesis, and applications. Chem. Mater. **26**(1), 123–133 (2013)
110. C. Sun, H. Li, L. Chen, Nanostructured ceria-based materials: synthesis, properties, and applications. Energy Environ. Sci. **5**(9), 8475–8505 (2012)
111. M.M. Khan, S.F. Adil, A. Al-Mayouf, *Metal Oxides as Photocatalysts* (Elsevier, Dordrecht, 2015)
112. K. Zhang, L. Guo, Metal sulphide semiconductors for photocatalytic hydrogen production. Catal. Sci. Technol. **3**(7), 1672–1690 (2013)
113. T. Di et al., Review on metal sulphide-based Z-scheme photocatalysts. ChemCatChem **11**(5), 1394–1411 (2019)
114. W. Shangguan, A. Yoshida, Photocatalytic hydrogen evolution from water on nanocomposites incorporating cadmium sulfide into the interlayer. J. Phys. Chem. B **106**(47), 12227–12230 (2002)
115. M.B. Tahir et al., Fabrication of heterogeneous photocatalysts for insight role of carbon nanofibre in hierarchical $WO_3/MoSe_2$ composite for enhanced photocatalytic hydrogen generation. Ceram. Int. **45**(5), 5547–5552 (2019)
116. T. Kanazawa et al., Structure and photocatalytic activity of $PdCrO_x$ cocatalyst on $SrTiO_3$ for overall water splitting. Catalysts **9**(1), 59 (2019)
117. Y. Nosaka, Y. Ishizuka, H. Miyama, Separation mechanism of a photoinduced electron-hole pair in metal-loaded semiconductor powders. Ber. Bunsenges. Phys. Chem. **90**(12), 1199–1204 (1986)
118. J.R. Darwent, G. Porter, Photochemical hydrogen production using cadmium sulphide suspensions in aerated water. J. Chem. Soc. Chem. Commun. **4**, 145–146 (1981)
119. M. Sathish, B. Viswanathan, R. Viswanath, Alternate synthetic strategy for the preparation of CdS nanoparticles and its exploitation for water splitting. Int. J. Hydrog. Energy **31**(7), 891–898 (2006)
120. J.S. Jang et al., Role of platinum-like tungsten carbide as cocatalyst of CdS photocatalyst for hydrogen production under visible light irradiation. Appl. Catal. A **346**(1–2), 149–154 (2008)
121. K. Kanade et al., Nano-CdS by polymer-inorganic solid-state reaction: visible light pristine photocatalyst for hydrogen generation. Mater. Res. Bull. **41**(12), 2219–2225 (2006)
122. Y. Li et al., Synthesis of CdS nanorods by an ethylenediamine assisted hydrothermal method for photocatalytic hydrogen evolution. J. Phys. Chem. C **113**(21), 9352–9358 (2009)
123. A. Sinha et al., Preparation of egg-shell type Al_2O_3-supported CdS photocatalysts for reduction of H_2O to H_2. Catal. Today **69**(1–4), 297–305 (2001)
124. M.K. Arora et al., Activity of cadmium sulfide photocatalysts for hydrogen production from water: role of support. Ind. Eng. Chem. Res. **38**(7), 2659–2665 (1999)
125. S. Shen et al., Effect of Ag_2S on solar-driven photocatalytic hydrogen evolution of nanostructured CdS. Int. J. Hydrog. Energy **35**(13), 7110–7115 (2010)
126. M. Subrahmanyam, V. Supriya, P.R. Reddy, Photocatalytic H_2 production with CdS-based catalysts from a sulphide/sulphite

substrate: an effort to develop MgO-supported catalysts. Int. J. Hydrog. Energy **21**(2), 99–106 (1996)
127. T. Kida et al., Photocatalytic hydrogen production from water over a $LaMnO_3$/CdS nanocomposite prepared by the reverse micelle method. J. Mater. Chem. **13**(5), 1186–1191 (2003)
128. Z. Shen et al., Sonochemistry synthesis of nanocrystals embedded in a MoO_3–CdS core–shell photocatalyst with enhanced hydrogen production and photodegradation. J. Mater. Chem. **22**(37), 19646–19651 (2012)
129. H. Fujii et al., Preparation and photocatalytic activities of a semiconductor composite of CdS embedded in a TiO_2 gel as a stable oxide semiconducting matrix. J. Mol. Catal. A: Chem. **129**(1), 61–68 (1998)
130. J.S. Jang et al., Fabrication of CdS/TiO_2 nano-bulk composite photocatalysts for hydrogen production from aqueous H_2S solution under visible light. Chem. Phys. Lett. **425**(4–6), 278–282 (2006)
131. J.S. Jang et al., Optimization of CdS/TiO_2 nano-bulk composite photocatalysts for hydrogen production from Na_2S/Na_2SO_3 aqueous electrolyte solution under visible light ($\lambda \geq 420$ nm). J. Photochem. Photobiol. A **188**(1), 112–119 (2007)
132. C. Li et al., TiO_2 nanotubes incorporated with CdS for photocatalytic hydrogen production from splitting water under visible light irradiation. Int. J. Hydrog. Energy **35**(13), 7073–7079 (2010)
133. X. Wang et al., Stable photocatalytic hydrogen evolution from water over ZnO–CdS core–shell nanorods. Int. J. Hydrog. Energy **35**(15), 8199–8205 (2010)
134. C. Xing et al., Band structure-controlled solid solution of $Cd_{1-x}Zn_xS$ photocatalyst for hydrogen production by water splitting. Int. J. Hydrog. Energy **31**(14), 2018–2024 (2006)
135. M.A. Fox, T.L. Pettit, Photoactivity of zeolite-supported cadmium sulfide: hydrogen evolution in the presence of sacrificial donors. Langmuir **5**(4), 1056–1061 (1989)
136. Y. Li et al., Photocatalytic hydrogen evolution over Pt/$Cd_{0.5}Zn_{0.5}S$ from saltwater using glucose as electron donor: an investigation of the influence of electrolyte NaCl. Int. J. Hydrog. Energy **36**(7), 4291–4297 (2011)
137. J. Yu, B. Yang, B. Cheng, Noble-metal-free carbon nanotube-$Cd_{0.1}Zn_{0.9}S$ composites for high visible-light photocatalytic H_2-production performance. Nanoscale **4**(8), 2670–2677 (2012)
138. H.C. Youn, S. Baral, J.H. Fendler, Dihexadecyl phosphate, vesicle-stabilized and in situ generated mixed cadmium sulfide and zinc sulfide semiconductor particles: preparation and utilization for photosensitized charge separation and hydrogen generation. J. Phys. Chem. **92**(22), 6320–6327 (1988)
139. A. Roy, G. De, Immobilisation of CdS, ZnS and mixed ZnS–CdS on filter paper: effect of hydrogen production from alkaline $Na_2S/Na_2S_2O_3$ solution. J. Photochem. Photobiol. A **157**(1), 87–92 (2003)
140. A. Koca, M. Şahin, Photocatalytic hydrogen production by direct sun light from sulfide/sulfite solution. Int. J. Hydrog. Energy **27**(4), 363–367 (2002)
141. X. Bai, J. Li, Photocatalytic hydrogen generation over porous $ZnIn_2S_4$ microspheres synthesized via a CPBr-assisted hydrothermal method. Mater. Res. Bull. **46**(7), 1028–1034 (2011)
142. S. Shen, L. Zhao, L. Guo, Cetyltrimethylammoniumbromide (CTAB)-assisted hydrothermal synthesis of $ZnIn_2S_4$ as an efficient visible-light-driven photocatalyst for hydrogen production. Int. J. Hydrog. Energy **33**(17), 4501–4510 (2008)
143. B. Chai et al., Preparation of a MWCNTs/$ZnIn_2S_4$ composite and its enhanced photocatalytic hydrogen production under visible-light irradiation. Dalton Trans. **41**(4), 1179–1186 (2012)
144. K. Zhang, Z. Zhou, L. Guo, Alkaline earth metal as a novel dopant for chalcogenide solid solution: improvement of photocatalytic efficiency of $Cd_{1-x}Zn_xS$ by barium surface doping. Int. J. Hydrog. Energy **36**(16), 9469–9478 (2011)
145. A. Bhirud et al., Surfactant tunable hierarchical nanostructures of $CdIn_2S_4$ and their photohydrogen production under solar light. Int. J. Hydrog. Energy **36**(18), 11628–11639 (2011)
146. B.B. Kale et al., $CdIn_2S_4$ nanotubes and "Marigold" nanostructures: a visible-light photocatalyst. Adv. Func. Mater. **16**(10), 1349–1354 (2006)
147. J.S. Jang et al., $AgGaS_2$-type photocatalysts for hydrogen production under visible light: effects of post-synthetic H2S treatment. J. Solid State Chem. **180**(3), 1110–1118 (2007)
148. D. Chen, J. Ye, Photocatalytic H_2 evolution under visible light irradiation on $AgIn_5S_8$ photocatalyst. J. Phys. Chem. Solids **68**(12), 2317–2320 (2007)
149. T. Arai et al., Cu-doped ZnS hollow particle with high activity for hydrogen generation from alkaline sulfide solution under visible light. Chem. Mater. **20**(5), 1997–2000 (2008)
150. M. Tabata et al., Photocatalytic hydrogen evolution from water using copper gallium sulfide under visible-light irradiation. J. Phys. Chem. C **114**(25), 11215–11220 (2010)
151. S.Y. Reece et al., Wireless solar water splitting using silicon-based semiconductors and earth-abundant catalysts. Science (2011). https://doi.org/10.1126/science.1209816
152. M.W. Kanan, D.G. Nocera, In situ formation of an oxygen-evolving catalyst in neutral water containing phosphate and Co^{2+}. Science **321**(5892), 1072–1075 (2008)
153. R.K. Hocking et al., Water-oxidation catalysis by manganese in a geochemical-like cycle. Nat. Chem. **3**(6), 461 (2011)
154. M.M. Najafpour, Oxygen evolving complex in Photosystem II: better than excellent. Dalton Trans. **40**(36), 9076–9084 (2011)
155. A. Zouni et al., Crystal structure of photosystem II from *Synechococcus elongatus* at 3.8 Å resolution. Nature **409**(6821), 739 (2001)
156. K.N. Ferreira et al., Architecture of the photosynthetic oxygen-evolving center. Science **303**(5665), 1831–1838 (2004)
157. A. Guskov et al., Cyanobacterial photosystem II at 2.9-Å resolution and the role of quinones, lipids, channels and chloride. Nat. Struct. Mol. Biol. **16**(3), 334 (2009)
158. M.M. Najafpour, A possible evolutionary origin for the Mn_4 cluster in photosystem II: from manganese superoxide dismutase to oxygen evolving complex. Orig. Life Evol. Biosph. **39**(2), 151–163 (2009)
159. Y. Nishiyama, S.I. Allakhverdiev, N. Murata, Protein synthesis is the primary target of reactive oxygen species in the photoinhibition of photosystem II. Physiol. Plant. **142**(1), 35–46 (2011)
160. K. Kawakami et al., Structure of the catalytic, inorganic core of oxygen-evolving photosystem II at 1.9 Å resolution. J. Photochem. Photobiol. B: Biol. **104**(1–2), 9–18 (2011)
161. Y. Umena et al., Crystal structure of oxygen-evolving photosystem II at a resolution of 1.9 Å. Nature **473**(7345), 55 (2011)
162. M.M. Najafpour, S.I. Allakhverdiev, Manganese compounds as water oxidizing catalysts for hydrogen production via water splitting: from manganese complexes to nano-sized manganese oxides. Int. J. Hydrog. Energy **37**(10), 8753–8764 (2012)
163. K. Mori, M. Dojo, H. Yamashita, Pd and Pd–Ag nanoparticles within a macroreticular basic resin: an efficient catalyst for hydrogen production from formic acid decomposition. Acs Catal. **3**(6), 1114–1119 (2013)
164. G. Nabi et al., Green synthesis of TiO_2 nanoparticles using lemon peel extract: their optical and photocatalytic properties. Int. J. Environ. Anal. Chem. (2020). https://doi.org/10.1080/03067319.2020.1722816
165. M. Rafique et al., Aquatic biodegradation of methylene blue by copper oxide nanoparticles synthesized from *Azadirachta indica* leaves extract. J. Inorg. Organomet. Polym Mater. **28**(6), 2455–2462 (2018)

166. K.E. Dekrafft, C. Wang, W. Lin, Metal-organic framework templated synthesis of Fe_2O_3/TiO_2 nanocomposite for hydrogen production. Adv. Mater. **24**(15), 2014–2018 (2012)
167. G.M. Scheuermann et al., Palladium nanoparticles on graphite oxide and its functionalized graphene derivatives as highly active catalysts for the Suzuki – Miyaura coupling reaction. J. Am. Chem. Soc. **131**(23), 8262–8270 (2009)
168. H. Zhang et al., P25-graphene composite as a high performance photocatalyst. ACS Nano **4**(1), 380–386 (2009)
169. Y. Zhang et al., TiO_2–graphene nanocomposites for gas-phase photocatalytic degradation of volatile aromatic pollutant: is TiO_2–graphene truly different from other TiO_2–carbon composite materials? ACS Nano **4**(12), 7303–7314 (2010)
170. G. Williams, B. Seger, P.V. Kamat, TiO_2-graphene nanocomposites. UV-assisted photocatalytic reduction of graphene oxide. ACS Nano **2**(7), 1487–1491 (2008)
171. W. Fan et al., Nanocomposites of TiO_2 and reduced graphene oxide as efficient photocatalysts for hydrogen evolution. J. Phys. Chem. C **115**(21), 10694–10701 (2011)
172. T. Peng et al., Enhanced photocatalytic hydrogen production over graphene oxide–cadmium sulfide nanocomposite under visible light irradiation. J. Phys. Chem. C **116**(43), 22720–22726 (2012)
173. H.-I. Kim et al., Solar photoconversion using graphene/TiO_2 composites: nanographene shell on TiO_2 core versus TiO_2 nanoparticles on graphene sheet. J. Phys. Chem. C **116**(1), 1535–1543 (2011)
174. Y. Zhang et al., Graphene transforms wide band gap ZnS to a visible light photocatalyst. The new role of graphene as a macromolecular photosensitizer. ACS Nano **6**(11), 9777–9789 (2012)
175. J. Zhang et al., Noble metal-free reduced graphene oxide-$Zn_xCd_{1-x}S$ nanocomposite with enhanced solar photocatalytic H_2-production performance. Nano Lett. **12**(9), 4584–4589 (2012)
176. A. Iwase et al., Reduced graphene oxide as a solid-state electron mediator in Z-scheme photocatalytic water splitting under visible light. J. Am. Chem. Soc. **133**(29), 11054–11057 (2011)
177. T. Di et al., Hierarchically CdS–Ag_2S nanocomposites for efficient photocatalytic H_2 production. Appl. Surf. Sci. **470**, 196–204 (2019)
178. M. Chandra, K. Bhunia, D. Pradhan, Controlled synthesis of CuS/TiO_2 heterostructured nanocomposites for enhanced photocatalytic hydrogen generation through water splitting. Inorg. Chem. **57**(8), 4524–4533 (2018)
179. H.Y. Hafeez et al., Ultrasound assisted synthesis of reduced graphene oxide (rGO) supported $InVO_4$-TiO_2 nanocomposite for efficient Hydrogen production. Ultrason. Sonochem. (2018). https://doi.org/10.1016/j.ultsonch.2018.12.009
180. H. Li et al., Mesoporous Au/TiO_2 nanocomposites with enhanced photocatalytic activity. J. Am. Chem. Soc. **129**(15), 4538–4539 (2007)
181. H. Liu, J. Zhang, D. Ao, Construction of heterostructured $ZnIn_2S_4$@ NH2-MIL-125 (Ti) nanocomposites for visible-light-driven H_2 production. Appl. Catal. B **221**, 433–442 (2018)
182. M. Pirhashemi, A. Habibi-Yangjeh, Facile fabrication of novel ZnO/$CoMoO_4$ nanocomposites: highly efficient visible-light-responsive photocatalysts in degradations of different contaminants. J. Photochem. Photobiol. A **363**, 31–43 (2018)
183. M. Mousavi, A. Habibi-Yangjeh, Magnetically recoverable highly efficient visible-light-active g-C_3N_4/Fe_3O_4/Ag_2WO_4/AgBr nanocomposites for photocatalytic degradations of environmental pollutants. Adv. Powder Technol. **29**(1), 94–105 (2018)
184. N. Qin et al., One-dimensional CdS/TiO_2 nanofiber composites as efficient visible-light-driven photocatalysts for selective organic transformation: synthesis, characterization, and performance. Langmuir **31**(3), 1203–1209 (2015)
185. S. Zhang et al., MoSSe nanotube: a promising photocatalyst with an extremely long carrier lifetime. J. Mater. Chem. A **7**, 7885–7890 (2019)
186. S. Yao et al., 2D Triphosphides: SbP_3 and GaP_3 monolayer as promising photocatalysts for water splitting. Int. J. Hydrog. Energy **44**, 5948–5954 (2019)
187. Q.H. Wang et al., Electronics and optoelectronics of two-dimensional transition metal dichalcogenides. Nat. Nanotechnol. **7**(11), 699 (2012)
188. B. Lu, X. Zheng, Z. Li, Few-layer P_4O_2: a promising photocatalyst for water splitting. ACS Appl. Mater. Interfaces **11**, 10163–10170 (2019)
189. M.B. Tahir et al., Role of $MoSe_2$ on nanostructures WO3-CNT performance for photocatalytic hydrogen evolution. Ceram. Int. **44**(6), 6686–6690 (2018)
190. A. Usman et al., Spectroscopic and structural dynamics of MoS_2 thin films. J. Nano Res. **58**, 74–79 (2019)
191. K.F. Mak et al., Atomically thin MoS_2: a new direct-gap semiconductor. Phys. Rev. Lett. **105**(13), 136805 (2010)
192. M. Bernardi, M. Palummo, J.C. Grossman, Extraordinary sunlight absorption and one nanometer thick photovoltaics using two-dimensional monolayer materials. Nano Lett. **13**(8), 3664–3670 (2013)
193. B. Hinnemann et al., Biomimetic hydrogen evolution: MoS_2 nanoparticles as catalyst for hydrogen evolution. J. Am. Chem. Soc. **127**(15), 5308–5309 (2005)
194. D. Voiry, J. Yang, M. Chhowalla, Recent strategies for improving the catalytic activity of 2D TMD nanosheets toward the hydrogen evolution reaction. Adv. Mater. **28**(29), 6197–6206 (2016)
195. C. Tsai et al., Active edge sites in $MoSe_2$ and WSe_2 catalysts for the hydrogen evolution reaction: a density functional study. Phys. Chem. Chem. Phys. **16**(26), 13156–13164 (2014)
196. S.M. Tan et al., Pristine basal and edge plane oriented molybdenite MoS_2 exhibiting highly anisotropic properties. Chem. A Eur. J. **21**(19), 7170–7178 (2015)
197. C. Tsai et al., Theoretical insights into the hydrogen evolution activity of layered transition metal dichalcogenides. Surf. Sci. **640**, 133–140 (2015)
198. M. Shao et al., Synergistic effect of 2D Ti_2C and gC_3N_4 for efficient photocatalytic hydrogen production. J. Mater. Chem. A **5**(32), 16748–16756 (2017)
199. F.A. Frame, F.E. Osterloh, CdSe-MoS_2: a quantum size-confined photocatalyst for hydrogen evolution from water under visible light. J. Phys. Chem. C **114**(23), 10628–10633 (2010)
200. X. Zong et al., Photocatalytic H_2 evolution on CdS loaded with WS_2 as cocatalyst under visible light irradiation. J. Phys. Chem. C **115**(24), 12202–12208 (2011)
201. G. Chen et al., A novel noble metal-free ZnS–WS_2/CdS composite photocatalyst for H_2 evolution under visible light irradiation. Catal. Commun. **40**, 51–54 (2013)
202. J. Chen et al., One-pot synthesis of CdS nanocrystals hybridized with single-layer transition-metal dichalcogenide nanosheets for efficient photocatalytic hydrogen evolution. Angew. Chem. **127**(4), 1226–1230 (2015)
203. M. Nguyen et al., In situ photo-assisted deposition of MoS_2 electrocatalyst onto zinc cadmium sulphide nanoparticle surfaces to construct an efficient photocatalyst for hydrogen generation. Nanoscale **5**(4), 1479–1482 (2013)
204. G. Tian et al., Enhanced photocatalytic hydrogen evolution over hierarchical composites of $ZnIn_2S_4$ nanosheets grown on MoS_2 slices. Chem. Asian J. **9**(5), 1291–1297 (2014)

205. W. Jiang et al., Photocatalytic hydrogen generation on bifunctional ternary heterostructured $In_2S_3/MoS_2/CdS$ composites with high activity and stability under visible light irradiation. J. Mater. Chem. A **3**(36), 18406–18412 (2015)
206. B. Mahler et al., Colloidal synthesis of 1T-WS_2 and 2H-WS_2 nanosheets: applications for photocatalytic hydrogen evolution. J. Am. Chem. Soc. **136**(40), 14121–14127 (2014)
207. M. Latorre-Sánchez et al., Innovative preparation of MoS2–graphene heterostructures based on alginate containing $(NH_4)2MoS_4$ and their photocatalytic activity for H_2 generation. Carbon **81**, 587–596 (2015)
208. S. Min, G. Lu, Sites for high efficient photocatalytic hydrogen evolution on a limited-layered MoS_2 cocatalyst confined on graphene sheets-the role of graphene. J. Phys. Chem. C **116**(48), 25415–25424 (2012)
209. Y. Hou et al., Photocatalytic hydrogen production over carbon nitride loaded with WS_2 as cocatalyst under visible light. Appl. Catal. B **156**, 122–127 (2014)

Muhammad Rafique is working as Assistant Professor in the University of Sahiwal, Sahiwal (Pakistan). He received a PhD in 2017 from University of Engineering and Technology, Lahore (Pakistan). His research interests include catalysis, wastewater treatments, water splitting and hydrogen production, supercapacitors, fuel cell, etc. He has published more than fifty research articles and numerous books in international journals and publishers of the fields.

Rikza Mubashar has completed her MPhil in Physics from the Department of Physics, University of Gujrat, Gujrat (Pakistan). She is working in material science under the supervision of Dr. Muhammad Rafique. Her research interests are materials synthesis and characterization for photocatalysis and supercapacitor.

Muneeb Irshad is an Assistant Professor in University of Engineering and Technology, Lahore (Pakistan). He completed his PhD degree in 2017 from University of Engineering and Technology, Lahore (Pakistan). His research interests include fabrication of solid oxide fuel cells, energy materials, pulsed laser deposition and laser-induced nanostructures.

S. S. A. Gillani is an Assistant Professor in the Government College University, Lahore (Pakistan). He completed his PhD in 2016 from Chemnitz University of Science and Technology, Germany. His research interests include computational materials science, catalysis and wastewater treatment.

M. Bilal Tahir is working as Faculty Member in the University of Gujrat, Gujrat (Pakistan). He completed his PhD from the University of Gujrat in 2018. His research interests include photocatalysis, dye degradation, water splitting, hydrogen evolution and carbon emissions. He has published a number of the research articles and books in his field.

N. R. Khalid is an Assistant Professor in the University of Gujrat, Gujrat (Pakistan). He completed his PhD in 2014 from Bahauddin Zikria University, Multan (Pakistan). He has specialization in the field of photocatalysis and hydrogen production and has published many research articles in his field.

Aqsa Yasmin is working as a product developer in the Advanced Materials and Membrane Technology Center, Punjab Industrial Estate, Kasur (Pakistan). She completed her PhD in 2019 from the University of Science and Technology of China. Her research interests include the development of electroactive charge storage and charge transport materials for batteries, water treatment, and catalysis.

M. Aamir Shehzad is working as a Lecturer in the University of Engineering and Technology, Lahore (Pakistan). He has completed his PhD in 2019 from the Universty of Science and Technology of China. He has specialization in conducting polymers and functional membranes for electrochemical devices. His research interests are advanced materials and polymers, conductive electroactive, photocatalytic water splitting, etc.